Finally, in *EGFR* mutant cell lines showing constitutive EGFR activation, we assessed how the mutations activate the tyrosine kinase domain of the receptor.

Materials and Methods

Cell lines. The human NSCLC cell lines NCI-H226 (H226), NCI-H292 (H292), NCI-H460 (H460), NCI-H1299 (H1299), NCI-H1650 (H1650), and NCI-H1975 (H1975) were obtained from the American Type Culture Collection (Manassas, VA). PC-9 and A549 cells were obtained as described previously (33). Ma-1 cells were kindly provided by E. Shimizu (Tottori University, Yonago, Japan). We established seven cell lines (KT-2, KT-4, Ma-25, Ma-31, Ma-34, Ma-45, and Ma-53) from tissue or pleural effusion of Japanese patients with advanced NSCLC. These cell lines were cultured under a humidified atmosphere of 5% CO_2 at 37°C in RPMI 1640 (Sigma, St. Louis, MO) supplemented with 10% fetal bovine serum. Informed consent for establishment of cell lines and tumor DNA sequencing was obtained in accordance with the ethical guidelines for human genome/genetic analysis in Japan.

Growth inhibition assay. Gefitinib was kindly provided by AstraZeneca (Macclesfield, United Kingdom) as a pure substance and was diluted in DMSO to obtain a stock solution of 20 mmol/L. For growth inhibition assays, cells (0.5×10^4 to 4.5×10^4) were plated in 96-well flat-bottomed plates and cultured for 24 h before the addition of various concentrations of gefitinib and incubation for an additional 72 h. TetraColor One (5 mmol/L tetrazolium monosodium salt and 0.2 mmol/L 1-methoxy-5-methyl phenazinium methylsulfate; Seikagaku, Tokyo, Japan) was then added to each well, and the cells were incubated for 3 h at 37°C before measurement of absorbance at 490 nm with a Multiskan Spectrum instrument (Thermo Labsystems, Boston, MA). Absorbance values were expressed as a percentage of that for untreated cells, and the concentration of gefitinib resulting in 50% growth inhibition (IC_{50}) was calculated.

Genetic analysis of *EGFR*. Genomic DNA was extracted from cell lines with the use of a QIAamp DNA Mini kit (Qiagen, Tokyo, Japan), and exons 18 to 21 of *EGFR* were amplified by the PCR and sequenced directly. PCR was done in a reaction mixture (25 μL) containing 50 ng of genomic DNA and TaKaRa Taq polymerase (TaKaRa BIO, Tokyo, Japan) and with an initial incubation for 3 min at 94°C followed by 30 cycles of 20 s at 94°C, 30 s at 58°C, and 20 s at 72°C and by a final incubation for 7 min at 72°C. The PCR products were purified with a Microcon YM-100 filtration device (Millipore, Billerica, MA) before sequencing with the use of an ABI BigDye Terminator v. 3.1 Cycle Sequencing kit (Applied Biosystems, Foster City, CA). Sequencing reaction mixtures were subjected to electrophoresis with an ABI PRISM 3100 Genetic Analyzer (Applied Biosystems). Primers for mutation analysis (sense and antisense, respectively) were as follows: exon 18, 5′-CAAATGAGCTGGCAAGTGCCGTGTC-3′ and 5′-GAGTTTCCCAAACACTCAGTGAAA-C-3′; exon 19, 5′-GCAATATCAGCCTTAGGTGCGGCTC-3′and 5′-CATAGAAAGTGAACATTTAGGATGTG-3′; exon 20, 5′-CCATGAGTACGTATTTTGAAACTC-3′ and 5′-CATATCCCCATGGCAAACTCTTGC-3′; and exon 21, 5′-CTAACGTTCGCCAGCCATAAGTCC-3′ and 5′-GCTGCGAGCTCACCCAGAATGTCTGG-3′.

FISH. *EGFR* copy number per cell was determined by FISH with the use of the LSI EGFR Spectrum Orange and CEP7 Spectrum Green probes (Vysis; Abbott, Des Plaines, IL). Cells were centrifuged onto glass slides with a Shandon cytocentrifuge (Thermo Electron, Pittsburgh, PA) and fixed by consecutive incubations with ice-cold 70% ethanol for 10 min, 85% ethanol for 5 min, and 100% ethanol for 5 min. Slides were stored at −20°C until analysis. Cells were subsequently subjected to digestion with pepsin for 10 min at 37°C, washed with water, dehydrated with a graded series of ethanol solutions, denatured with 70% formamide in 2× SSC for 5 min at 72°C, and dehydrated again with a graded series of ethanol solutions before incubation with a hybridization mixture consisting of 50% formamide, 2× SSC, Cot-1 DNA, and labeled DNA. The slides were washed for 5 min at 73°C with 3× SSC, for 5 min at 37°C with 4× SSC containing 0.1% Triton X-100, and for 5 min at room temperature with 2× SSC before counterstaining with antifade solution containing 4′,6-diamidino-2-phenylindole. Hybridization signals were scored in 40 nuclei with the use of a ×100 immersion objective. Nuclei with a disrupted boundary were excluded from the analysis. Gene amplification was defined by an *EGFR*/chromosome 7 copy number ratio of ≥2 or by the presence of clusters of ≥15 copies of *EGFR* per cell in ≥10% of cells, as described previously (25, 27).

Immunoblot analysis. Cell lysates were fractionated by SDS-PAGE on a 7.5% gel, and the separated proteins were transferred to a nitrocellulose membrane. After blocking of nonspecific sites with 5% skim milk, the membrane was incubated overnight at room temperature with primary antibodies. Antibodies to phosphorylated EGFR (pY845, pY1068, or pY1173), extracellular signal-regulated kinase (ERK), phosphorylated AKT, AKT, Src homology and collagen (Shc), and phosphorylated Shc were obtained from Cell Signaling Technology (Beverly, MA); antibodies to EGFR were from Zymed (South San Francisco, CA); antibodies to phosphorylated ERK were from Santa Cruz Biotechnology (Santa Cruz, CA); and antibodies to β-actin (loading control) were from Sigma. Immune complexes were detected by incubation of the membrane for 1 h at room temperature with horseradish peroxidase–conjugated goat antibodies to mouse or rabbit immunoglobulin (Amersham Biosciences, Little Chalfont, United Kingdom) and by subsequent exposure to enhanced chemiluminescence reagents (Perkin-Elmer, Boston, MA).

Table 1. Characteristics of NSCLC cell lines

Cell lines	Gefitinib IC_{50} (μmol/L)	*EGFR* mutation	*EGFR* amplification	Histology
PC-9	0.07	del(E746-A750)	+	Adenocarcinoma
KT-2	0.57	L858R	+	Adenocarcinoma
KT-4	1.26	L858R	+	Large cell carcinoma
Ma-1	2.34	del(E746-A750)	+	Adenocarcinoma
H1650	6.66	del (E746-A750)	−	Adenocarcinoma
A549	8.70	Wild type	−	Adenocarcinoma
H1975	9.32	L858R+T790M	−	Adenocarcinoma
H292	9.44	Wild type	−	Mucoepidermoid carcinoma
H226	9.53	Wild type	−	Squamous cell carcinoma
Ma-25	10.17	Wild type	−	Large cell carcinoma
H460	10.38	Wild type	−	Large cell carcinoma
Ma-45	10.47	Wild type	−	Adenocarcinoma
Ma-53	10.47	Wild type	−	Adenocarcinoma
Ma-34	11.17	Wild type	−	Adenocarcinoma
H1299	11.28	Wild type	−	Large cell carcinoma
Ma-31	12.46	Wild type	−	Adenocarcinoma

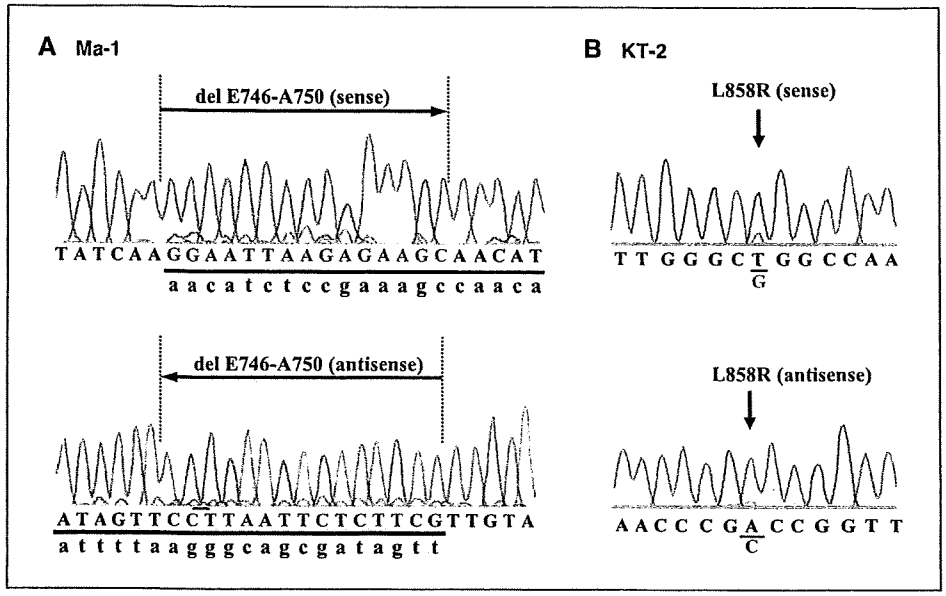

Figure 1. Detection of *EGFR* mutations in NSCLC cell lines. The portions of the sequencing electrophoretograms corresponding to the mutations are shown for Ma-1 (*A*) and KT-2 (*B*) cells. *A*, heterozygous in-frame deletion in exon 19 is revealed by the presence of double peaks. Tracings in both sense and antisense directions are shown to highlight the two breakpoints of the deletion. Wild-type (*uppercase*) and mutant (*lowercase*) nucleotide sequences. *B*, heterozygous point mutation (T → G) at nucleotide position 2819 in exon 21.

Treatment of cells with neutralizing antibodies. Cells were exposed to neutralizing antibodies (each at 12 μg/mL) for 3 h before EGF stimulation. The antibodies included those to EGF and to transforming growth factor-α (TGF-α), both from R&D Systems (Minneapolis, MN) as well as antibodies to EGFR (Upstate Biotechnology, Lake Placid, NY). Cell lysates were then prepared and subjected to immunoblot analysis with antibodies to phosphorylated EGFR (pY1068) and to EGFR as described above.

Chemical cross-linking assay. Chemical cross-linking was done as described previously (34, 35). Cells were washed twice with ice-cold PBS and then incubated for 20 min at 4°C with 1 mmol/L bis(sulfosuccinimidyl)-suberate (Pierce, Rockford, IL) in PBS. The cross-linking reaction was terminated by the addition of glycine to a final concentration of 250 mmol/L and incubation for an additional 5 min at 4°C. The cells were washed with PBS, and cell lysates were resolved by SDS-PAGE on a 4% gel and subjected to immunoblot analysis with anti-EGFR (Santa Cruz Biotechnology).

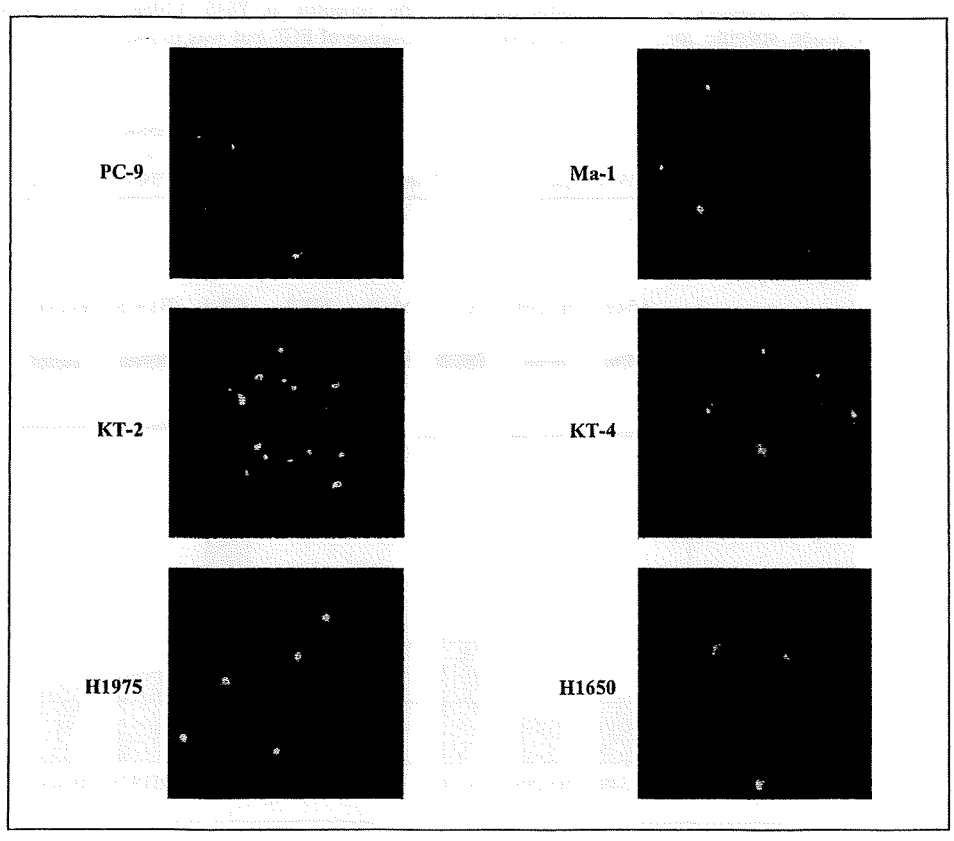

Figure 2. FISH analysis of *EGFR* amplification in NSCLC cell lines. The analysis was done with probes specific for *EGFR* (*red signals*) and for the centromere of chromosome 7 (*green signals*) in the indicated cell lines. PC-9 and Ma-1 cells manifest an *EGFR*/chromosome copy number ratio of ≥2, whereas KT-2 and KT-4 cells manifest *EGFR* clusters. H1975 and H1650 cells are negative for *EGFR* amplification.

Results

Effect of gefitinib on the growth of NSCLC cell lines. We first examined the effect of the EGFR-TKI gefitinib on the growth of 16 NSCLC cell lines, eight of which (KT-2, KT-4, Ma-1, Ma-25, Ma-31, Ma-34, Ma-45, and Ma-53) were established from Japanese NSCLC patients for the present study. The IC_{50} values for gefitinib chemosensitivity ranged from 0.07 to 12.46 μmol/L (a 178-fold difference; Table 1).

Four cell lines (PC-9, KT-2, KT-4, and Ma-1) were relatively sensitive to gefitinib with IC_{50} values between 0.07 and 2.34 μmol/L, whereas the remaining 12 lines were considered resistant to gefitinib (IC_{50} > 6 μmol/L). No relation was apparent between sensitivity to gefitinib and histologic subtype of NSCLC for this panel of cell lines (Table 1).

***EGFR* mutation and amplification in NSCLC cell lines.** We screened the 16 NSCLC cell lines for the presence of *EGFR* mutations in exons 18 to 21, which encode the catalytic domain of the receptor. As previously described (36–39), PC-9, H1650, and H1975 cell lines were found to harbor *EGFR* mutations [del(E746-A750) in PC-9 and H1650 and both L858R and T790M in H1975]. Furthermore, we detected *EGFR* mutations in three of the newly established cell lines (Ma-1, KT-2, and KT-4). Ma-1 cells, which were isolated from a female ex smoker with adenocarcinoma (>30 years of age), were found to harbor a small deletion within exon 19 [del(E746-A750); Fig. 1*A*; Table 1]. Both KT-2 cells [derived from a male ex smoker with adenocarcinoma (>30 years of age)] and KT-4 cells (derived from a male nonsmoker with large cell carcinoma) harbor a point mutation (L858R) in exon 21 (Fig. 1*B*; Table 1). Four of these six NSCLC cell lines with *EGFR* mutations (PC-9, Ma-1, KT-2, and KT-4) are sensitive to gefitinib (Table 1), consistent with clinical observations (15–17, 20, 22).

We next examined the 16 NSCLC cell lines for the presence of *EGFR* amplification by FISH analysis with a probe specific for *EGFR* and a control probe for the centromere of chromosome 7. Four (PC-9, Ma-1, KT-2, and KT-4) of the 16 cell lines, all of which harbor *EGFR* mutations, were found to be positive for *EGFR* amplification (Fig. 2; Table 1). PC-9 and Ma-1 cell lines, both of which harbor the same exon 19 deletion, showed an *EGFR*/chromosome copy number ratio of ≥2, whereas KT-2 and KT-4, both of which harbor the L858R mutation in exon 21, showed a clustered unbalanced gain of *EGFR* copy number (Fig. 2). The four cell lines that manifested both *EGFR* mutation and amplification were sensitive to gefitinib (Table 1). The *EGFR* mutant cell lines H1650 and H1975 showed no evidence of *EGFR* amplification (Fig. 2), and both of these lines were relatively resistant to gefitinib (Table 1). None of the cell lines negative for *EGFR* mutations manifested *EGFR* amplification (Table 1), suggesting that *EGFR* mutation is closely associated with *EGFR* amplification ($P < 0.05$, χ^2 test).

EGFR expression in NSCLC cell lines. We examined the basal abundance of EGFR in *EGFR* wild-type and mutant NSCLC cell lines by immunoblot analysis. The amount of EGFR in the cell lines PC-9, Ma-1, KT-2, and KT-4, all of which manifest *EGFR* amplification and *EGFR* mutation, was increased compared with that in *EGFR* wild-type cell lines (A549 and H1299) or *EGFR* mutant cell lines negative for *EGFR* amplification (H1975 and H1650; Fig. 3). These results, thus, reveal a close relation between increased EGFR expression and *EGFR* amplification in this panel of NSCLC cell lines, consistent with the results of previous analyses of NSCLC tissue specimens (6, 7).

EGFR phosphorylation in NSCLC cell lines. We examined tyrosine phosphorylation of endogenous EGFRs in NSCLC cell lines by immunoblot analysis with phosphorylation site–specific antibodies. In cells (A549) that express only wild-type EGFR, phosphorylation of the receptor at Y845, Y1068, or Y1173 was undetectable in the absence of EGF but was markedly induced on

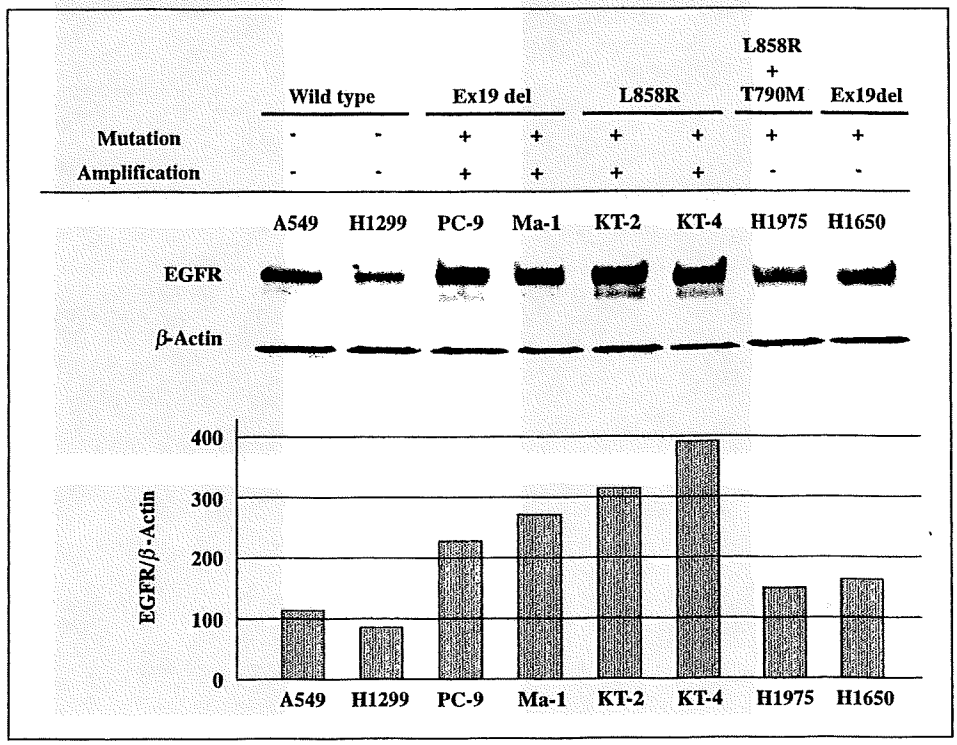

Figure 3. EGFR expression in NSCLC cell lines. Lysates (40 μg of protein) of NSCLC cell lines positive or negative for *EGFR* mutation or amplification, as indicated, were subjected to immunoblot analysis with antibodies to EGFR and to β-actin (*top*). The abundance of EGFR relative to that of β-actin was determined by densitometry (*bottom*). Representative of three independent experiments.

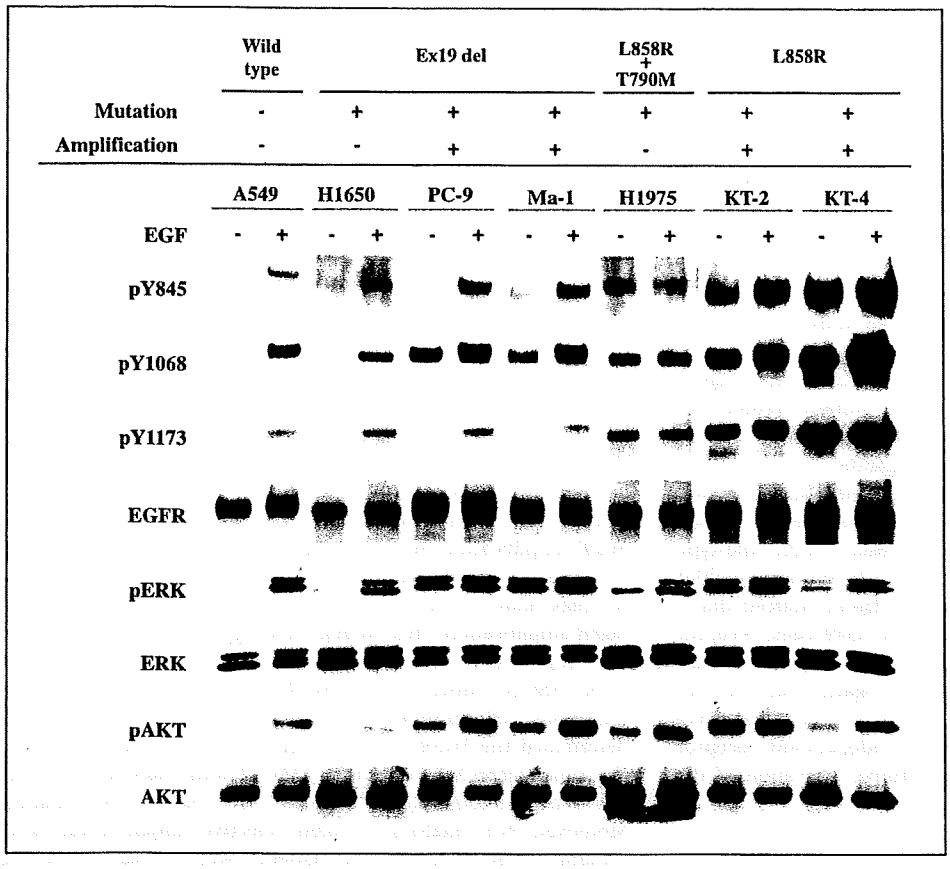

Figure 4. Phosphorylation of EGFR and downstream signaling molecules in NSCLC cell lines. Serum-deprived cells were incubated for 15 min in the absence or presence of EGF (100 ng/mL), after which cell lysates (40 μg of protein) were subjected to immunoblot analysis with antibodies to phosphorylated forms of EGFR (*pEGFR*), ERK (*pERK*), or AKT (*pAKT*) as well as antibodies to all forms of the corresponding proteins, as indicated. Representative of three independent experiments.

exposure of the cells to this growth factor (Fig. 4). Similar results were obtained with H1650 cells, which are positive for the deletion in exon 19 of *EGFR* but negative for *EGFR* amplification. In contrast, PC-9 and Ma-1 cells, which are positive for both the exon 19 deletion and *EGFR* amplification, manifested an increased basal level of EGFR phosphorylation at Y1068, indicative of constitutive activation of the EGFR tyrosine kinase. Exposure of PC-9 or Ma-1 cells to EGF induced EGFR phosphorylation at Y845 and Y1173, showing that the mutant receptors remain sensitive to ligand stimulation. Furthermore, the cell lines (H1975, KT-2, and KT-4) with the L858R point mutation manifested an increased basal level of EGFR phosphorylation at Y845, Y1068, and Y1173, and the extent of phosphorylation at these residues was increased only slightly by treatment of the cells with EGF, indicative of constitutive activation of the EGFR tyrosine kinase. These results thus showed that endogenous *EGFR* mutations result in constitutive receptor activation, and that the patterns of tyrosine phosphorylation of EGFR differ between the two most common types of *EGFR* mutant.

Phosphorylation of signaling molecules downstream of EGFR in NSCLC cell lines. Given that constitutive activation of EGFR was detected in NSCLC cell lines with endogenous *EGFR* mutations, we examined whether signaling molecules that act downstream of the receptor are also constitutively activated in these cell lines. We first examined the basal levels of phosphorylation of AKT and ERK, both of which mediate the oncogenic effects of EGFR. Immunoblot analysis with antibodies to phosphorylated forms of AKT or ERK revealed that these molecules are indeed constitutively activated in the *EGFR* mutant lines (PC-9, Ma-1, H1975, KT-2, and KT-4) that manifest constitutive activation of EGFR, although the extent of phosphorylation varied (Fig. 4). The increased levels of AKT and ERK phosphorylation in these mutant cell lines are consistent with the increased level of EGFR phosphorylation on Y1068, which serves as the docking site for phosphatidylinositol 3-kinase and growth factor receptor binding protein 2, molecules that mediate the activation of AKT and the Ras-ERK pathway, respectively (2, 40). We next examined whether the differences in the pattern of constitutive tyrosine phosphorylation of EGFR apparent between NSCLC cell lines harboring the exon 19 deletion and those with the L858R mutation in exon 21 are associated with distinct alterations in downstream signaling pathways. Given that Y1173, a major docking site of EGFR for the adapter protein Shc (2, 40, 41), is constitutively phosphorylated in cells with the L858R mutation but not in those with the exon 19 deletion, we compared Shc phosphorylation between cell lines with these two types of *EGFR* mutation. Ligand-independent tyrosine phosphorylation of the 52- and 46-kDa isoforms of Shc was apparent in cell lines with either type of *EGFR* mutation (Fig. 5). However, cell lines (KT-2 and KT-4) that harbor the L858R mutation exhibited a markedly greater basal level of phosphorylation of the 66-kDa isoform of Shc than did those (PC-9 and Ma-1) that harbor the exon 19 deletion or those (A549) that harbor only wild-type *EGFR*. These data suggest that the constitutively active mutant forms of *EGFR* induce selective activation of downstream effectors as a result of differential patterns of receptor autophosphorylation.

Ligand-independent dimerization and activation of *EGFR* mutants. Evidence suggests that EGFR ligands, including EGF and TGF-α, secreted by tumor cells themselves might be responsible for activation of mutant receptors in an autocrine loop (29, 42). To investigate whether EGFR is constitutively activated as a result of such an autocrine mechanism in *EGFR* mutant NSCLC cell lines, we treated the cells with a combination of three neutralizing antibodies (anti-EGF, anti–TGF-α, and anti-EGFR) for 3 h and then examined the effect of EGF on EGFR phosphorylation. The ligand-dependent activation of EGFR in A549 cells (which express only wild-type *EGFR*) was blocked by such antibody treatment (Fig. 6*A*). In contrast, treatment of the *EGFR* mutant cell lines PC-9 or KT-4 with the neutralizing antibodies failed to inhibit the constitutive phosphorylation of EGFR on Y1068. These observations suggest that the constitutive phosphorylation of the mutant receptors is not attributable to autocrine stimulation, although we are not able to exclude a possible role for other EGFR ligands.

Ligand-induced EGFR dimerization is responsible for activation of the receptor tyrosine kinase (4, 5). To determine whether mutant receptors are constitutively dimerized, we treated *EGFR* wild-type or mutant cell lines with a cross-linking agent before immunoblot analysis with antibodies to EGFR. Whereas ligand-induced dimerization of wild-type *EGFR* was observed in A549 cells, receptor dimerization in PC-9 and KT-4 cells, which express mutant receptors, was apparent in the absence of ligand and was not increased substantially by exposure of the cells to EGF (Fig. 6*B*). These data indicate that ligand-independent receptor dimerization is responsible for the constitutive activation of the mutant forms of *EGFR*.

Discussion

The discovery of somatic mutations in the tyrosine kinase domain of EGFR and of their association with a high response rate to EGFR-TKIs has had a substantial effect on the treatment of advanced NSCLC (15–17, 20, 22). Asian patients with NSCLC seem to have a higher prevalence of these mutations, ranging from 20% to 40% (18, 20, 21, 43–45). We have now identified *EGFR* mutations in three of eight newly established cell lines from Japanese patients with advanced NSCLC. Characterization of these eight new cell lines and eight previously established NSCLC lines revealed that, consistent with previous observations (29, 31, 36), those cell lines that harbor *EGFR* mutations are more likely to be sensitive to gefitinib than are those without such mutations. Not all *EGFR* mutant cell lines (e.g., H1650 and H1975) are sensitive to this EGFR-TKI, however, suggesting the existence of additional determinants of gefitinib sensitivity. In addition to the L858R mutation in exon 21 of *EGFR*, H1975 cells contain the T790M mutation in exon 20, which has been shown to confer resistance to EGFR-TKIs (38, 39). H1650 cells, which do not harbor mutations in *EGFR* other than the exon 19 deletion, manifest loss of the tumor suppressor phosphatase and tensin homologue deleted on chromosome 10 (37), which may result in resistance to EGFR-TKIs. *EGFR* amplification in NSCLC cells has also been shown to correlate with a better response to gefitinib (22, 25–27). Given that little is known of the relation between *EGFR* mutation and amplification in NSCLC, we examined the 16 NSCLC cell lines used in this study for *EGFR* amplification by FISH. Four of the six cell lines with *EGFR* mutations were found to be positive for gene amplification, whereas none of the 10 mutation-negative cell lines manifested *EGFR* amplification. This finding thus suggests that *EGFR* mutation and amplification are linked. Cappuzzo et al. showed that 6 of 9 (67%) NSCLC patients with *EGFR* amplification also had *EGFR* mutations (25). Furthermore, Takano et al. sequenced *EGFR* and determined the *EGFR* copy number by real-time PCR analysis for the tumors of 66 NSCLC patients (22); all of the patients with a high *EGFR* copy number (≥6.0 per cell) also had *EGFR* mutations. Moreover, PCR analysis revealed selective amplification of the mutant *EGFR* alleles in the patients with a high *EGFR* copy number. Our sequencing electrophoretograms for the *EGFR* mutant cell lines positive for *EGFR* amplification also revealed that the mutant signals were dominant, and the wild-type sequence was barely detectable (Fig. 1), indicative of selective amplification of the mutant alleles. We used the recently proposed definition of *EGFR* amplification as determined by FISH (25, 27) and found that the pattern of gene amplification seemed to be dependent on the

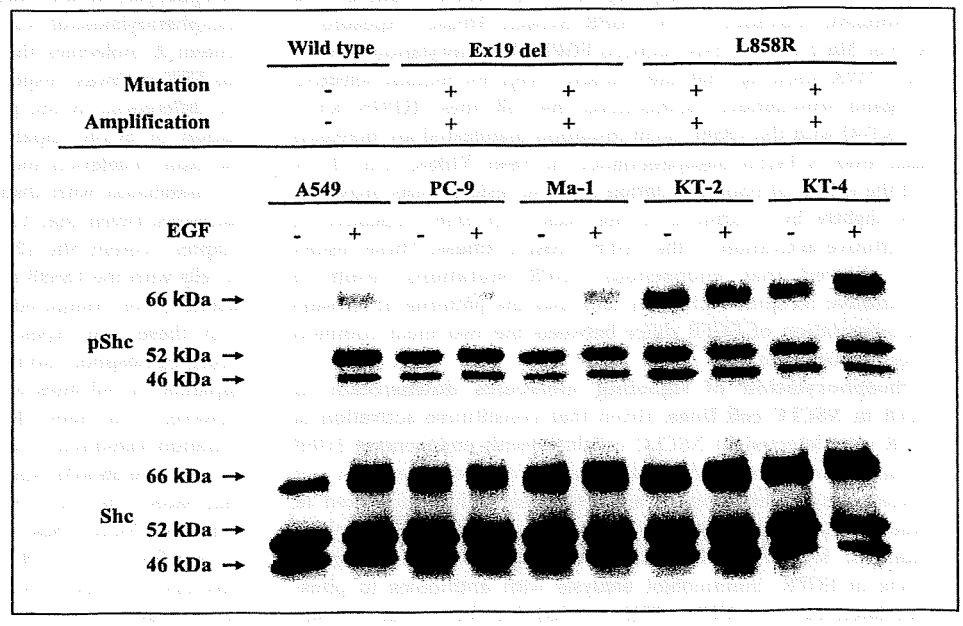

Figure 5. Phosphorylation of Shc in NSCLC cell lines. Serum-deprived cells were incubated for 15 min in the absence or presence of EGF (100 ng/mL), after which cell lysates (40 μg of protein) were subjected to immunoblot analysis with antibodies to phosphorylated Shc (*pShc*) or total Shc. Representative of three independent experiments.

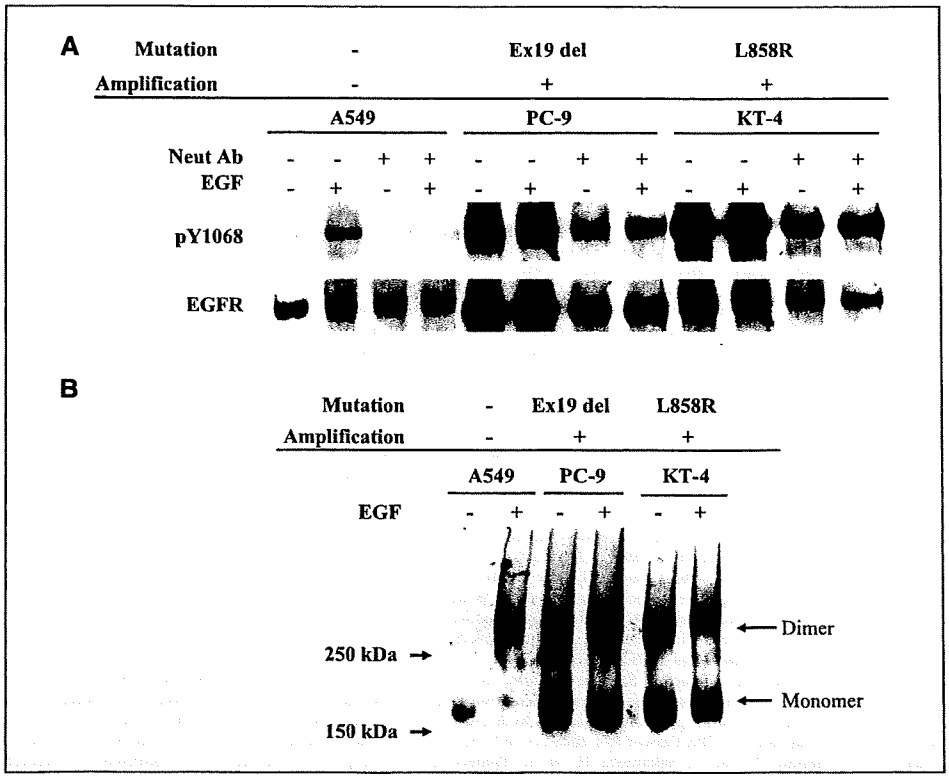

Figure 6. Mechanism of constitutive activation of EGFR in NSCLC cell lines. *A*, effect of neutralizing antibodies (*Neut Ab*) on EGFR phosphorylation. Serum-deprived NSCLC cells (A549, PC-9, or KT-4) were incubated for 3 h with a combination of neutralizing antibodies to EGF, TGF-α, and EGFR and then for 15 min in the additional absence or presence of EGF (100 ng/mL). Cell lysates were then prepared and subjected to immunoblot analysis with antibodies to the Y1068-phosphorylated form of EGFR or to total EGFR. *B*, EGFR dimerization. Serum-deprived cells were incubated for 15 min in the absence or presence of EGF (100 ng/mL), exposed to a chemical cross-linker, lysed, and subjected to immunoblot analysis with antibodies to EGFR. Representative of three independent experiments.

type of *EGFR* mutation; gene clusters were observed in cells with the L858R mutation in exon 21, whereas an *EGFR*/chromosome copy number ratio of ≥2 was detected in those with the small deletion [del(E746-A750)] in exon 19. Together, these data support the notion that *EGFR* mutation and amplification may be co-selected for during the growth of NSCLC cells. The four cell lines (PC-9, Ma-1, KT-2, and KT-4) positive for both *EGFR* mutation and amplification were sensitive to gefitinib, suggesting that *EGFR* amplification may increase sensitivity to gefitinib in *EGFR* mutant cells.

Previous biochemical studies of cells transiently transfected with vectors for wild-type or mutant forms of EGFR suggested that *EGFR* mutations increase EGF-dependent receptor activation (15, 30). Infection of NIH 3T3 cells with a retrovirus encoding *EGFR* mutants showed that the mutant receptors are constitutively activated and able to induce cell transformation in the absence of exogenous EGF (32). We examined the activation status of endogenous EGFRs in the six NSCLC cell lines that harbor *EGFR* mutations. The H1650, PC-9, and Ma-1 cell lines, all of which harbor the same exon 19 deletion, showed different patterns of EGFR autophosphorylation in the COOH-terminal region of the protein. EGFR autophosphorylation was ligand dependent in H1650 cells, which are negative for *EGFR* amplification, whereas Y1068 (but not Y845 and Y1173) was constitutively phosphorylated in PC-9 and Ma-1 cells, both of which manifest *EGFR* amplification. These results suggest that both *EGFR* mutation and amplification may be required for constitutive activation of EGFR in NSCLC cells that harbor the exon 19 deletion. In contrast, NSCLC cell lines (H1975, KT-2, and KT-4) that harbor the L858R mutation exhibited constitutive phosphorylation of EGFR at Y845, Y1068, and Y1173, regardless of the absence or presence of *EGFR* amplification. It is thought that *EGFR* mutations result in repositioning of critical residues surrounding the ATP-binding cleft of the tyrosine kinase domain of the receptor and thereby stabilize the interactions with ATP and EGF-TKIs, leading to increased tyrosine kinase activity and EGFR-TKI sensitivity (15, 23, 24). The differential activation of *EGFR* mutants observed in the present study may result from distinct conformational changes within the catalytic pocket caused by the different types of *EGFR* mutation. NSCLC patients with exon 19 deletions were recently shown to manifest longer overall survival than did those with the exon 21 point mutation after treatment with EGFR-TKIs, supporting the notion that the two major types of mutant receptors have different biological properties (46, 47).

Ligand-induced receptor dimerization underlies the activation of receptor tyrosine kinases (4, 5). Chemical cross-linking revealed that EGF binding to EGFR induced receptor dimerization in A549 cells, which express only the wild-type form of the receptor. In contrast, endogenous EGFRs in NSCLC cells harboring either the exon 19 deletion or the point mutation in exon 21 of *EGFR* were found to dimerize in the absence of ligand, suggesting that the constitutive activation of the mutant receptors is attributable to ligand-independent dimerization. EGFR dimerization was shown to be induced by interaction of quinazolines with the ATP-binding site of the receptor in the absence of ligand binding, suggesting that a change in conformation around the ATP-binding pocket of EGFR is sufficient for receptor dimerization (35). Conformational changes induced by *EGFR* mutations may therefore also trigger EGFR dimerization in *EGFR* mutant cells.

In conclusion, we have found that *EGFR* mutation is closely associated with *EGFR* amplification in NSCLC cell lines. Endogenous EGFRs expressed in NSCLC cells positive for both *EGFR* mutation and amplification are constitutively activated as a result

of ligand-independent dimerization. Cells with the two most common types of *EGFR* mutation also manifest different patterns of EGFR autophosphorylation. Prospective studies are required to determine the potential for exploitation of these *EGFR* alterations in the treatment of advanced NSCLC.

Acknowledgments

Received 9/12/2006; revised 10/30/2006; accepted 12/10/2006.

The costs of publication of this article were defrayed in part by the payment of page charges. This article must therefore be hereby marked *advertisement* in accordance with 18 U.S.C. Section 1734 solely to indicate this fact.

We thank Takeko Wada, Erina Hatashita, and Yuki Yamada for technical assistance.

References

1. Wang Y, Minoshima S, Shimizu N. Precise mapping of the EGF receptor gene on the human chromosome 7p12 using an improved FISH technique. Jpn J Hum Genet 1993;38:399–406.
2. Jorissen RN, Walker F, Pouliot N, Garrett TP, Ward CW, Burgess AW. Epidermal growth factor receptor: mechanisms of activation and signalling. Exp Cell Res 2003; 284:31–53.
3. Hynes NE, Lane HA. ERBB receptors and cancer: the complexity of targeted inhibitors. Nat Rev Cancer 2005; 5:341–54.
4. Ogiso H, Ishitani R, Nureki O, et al. Crystal structure of the complex of human epidermal growth factor and receptor extracellular domains. Cell 2002;110:775–87.
5. Schlessinger J. Ligand-induced, receptor-mediated dimerization and activation of EGF receptor. Cell 2002;110:669–72.
6. Hirsch FR, Varella-Garcia M, Bunn PA, Jr., et al. Epidermal growth factor receptor in non-small-cell lung carcinomas: correlation between gene copy number and protein expression and impact on prognosis. J Clin Oncol 2003;21:3798–807.
7. Suzuki S, Dobashi Y, Sakurai H, Nishikawa K, Hanawa M, Ooi A. Protein overexpression and gene amplification of epidermal growth factor receptor in nonsmall cell lung carcinomas. An immunohistochemical and fluorescence *in situ* hybridization study. Cancer 2005;103: 1265–73.
8. Shepherd FA, Rodrigues Pereira J, Ciuleanu T, et al. Erlotinib in previously treated non-small-cell lung cancer. N Engl J Med 2005;353:123–32.
9. Thatcher N, Chang A, Parikh P, et al. Gefitinib plus best supportive care in previously treated patients with refractory advanced non-small-cell lung cancer: results from a randomised, placebo-controlled, multicentre study (Iressa Survival Evaluation in Lung Cancer). Lancet 2005;366:1527–37.
10. Fukuoka M, Yano S, Giaccone G, et al. Multi-institutional randomized phase II trial of gefitinib for previously treated patients with advanced non-small-cell lung cancer (the IDEAL 1 trial). J Clin Oncol 2003;21: 2237–46.
11. Kaneda H, Tamura K, Kurata T, Uejima H, Nakagawa K, Fukuoka M. Retrospective analysis of the predictive factors associated with the response and survival benefit of gefitinib in patients with advanced non-small-cell lung cancer. Lung Cancer 2004;46:247–54.
12. Takano T, Ohe Y, Kusumoto M, et al. Risk factors for interstitial lung disease and predictive factors for tumor response in patients with advanced non-small cell lung cancer treated with gefitinib. Lung Cancer 2004;45:93–104.
13. Tamura K, Fukuoka M. Gefitinib in non-small cell lung cancer. Expert Opin Pharmacother 2005;6:985–93.
14. Ando M, Okamoto I, Yamamoto N, et al. Predictive factors for interstitial lung disease, antitumor response, and survival in non-small-cell lung cancer patients treated with gefitinib. J Clin Oncol 2006;24:2549–56.
15. Lynch TJ, Bell DW, Sordella R, et al. Activating mutations in the epidermal growth factor receptor underlying responsiveness of non-small-cell lung cancer to gefitinib. N Engl J Med 2004;350:2129–39.
16. Paez JG, Janne PA, Lee JC, et al. EGFR mutations in lung cancer: correlation with clinical response to gefitinib therapy. Science 2004;304:1497–500.
17. Pao W, Miller V, Zakowski M, et al. EGF receptor gene mutations are common in lung cancers from "never smokers" and are associated with sensitivity of tumors to gefitinib and erlotinib. Proc Natl Acad Sci U S A 2004; 101:13306–11.
18. Kosaka T, Yatabe Y, Endoh H, Kuwano H, Takahashi T, Mitsudomi T. Mutations of the epidermal growth factor receptor gene in lung cancer: biological and clinical implications. Cancer Res 2004; 64:8919–23.
19. Han SW, Kim TY, Hwang PG, et al. Predictive and prognostic impact of epidermal growth factor receptor mutation in non-small-cell lung cancer patients treated with gefitinib. J Clin Oncol 2005;23:2493–501.
20. Mitsudomi T, Kosaka T, Endoh H, et al. Mutations of the epidermal growth factor receptor gene predict prolonged survival after gefitinib treatment in patients with non-small-cell lung cancer with postoperative recurrence. J Clin Oncol 2005;23:2513–20.
21. Tokumo M, Toyooka S, Kiura K, et al. The relationship between epidermal growth factor receptor mutations and clinicopathologic features in non-small cell lung cancers. Clin Cancer Res 2005;11:1167–73.
22. Takano T, Ohe Y, Sakamoto H, et al. Epidermal growth factor receptor gene mutations and increased copy numbers predict gefitinib sensitivity in patients with recurrent non-small-cell lung cancer. J Clin Oncol 2005;23:6829–37.
23. Gazdar AF, Shigematsu H, Herz J, Minna JD. Mutations and addiction to EGFR: the Achilles 'heal' of lung cancers? Trends Mol Med 2004;10:481–6.
24. Shigematsu H, Gazdar AF. Somatic mutations of epidermal growth factor receptor signaling pathway in lung cancers. Int J Cancer 2006;118:257–62.
25. Cappuzzo F, Hirsch FR, Rossi E, et al. Epidermal growth factor receptor gene and protein and gefitinib sensitivity in non-small-cell lung cancer. J Natl Cancer Inst 2005;97:643–55.
26. Hirsch FR, Varella-Garcia M, McCoy J, et al. Increased epidermal growth factor receptor gene copy number detected by fluorescence *in situ* hybridization associates with increased sensitivity to gefitinib in patients with bronchioloalveolar carcinoma subtypes: a Southwest Oncology Group Study. J Clin Oncol 2005;23:6838–45.
27. Tsao MS, Sakurada A, Cutz JC, et al. Erlotinib in lung cancer: molecular and clinical predictors of outcome. N Engl J Med 2005;353:133–44.
28. Ishikawa N, Daigo Y, Takano A, et al. Increases of amphiregulin and transforming growth factor-α in serum as predictors of poor response to gefitinib among patients with advanced non-small cell lung cancers. Cancer Res 2005;65:9176–84.
29. Tracy S, Mukohara T, Hansen M, Meyerson M, Johnson BE, Janne PA. Gefitinib induces apoptosis in the EGFRL858R non-small-cell lung cancer cell line H3255. Cancer Res 2004;64:7241–4.
30. Sordella R, Bell DW, Haber DA, Settleman J. Gefitinib-sensitizing EGFR mutations in lung cancer activate anti-apoptotic pathways. Science 2004;305:1163–7.
31. Amann J, Kalyankrishna S, Massion PP, et al. Aberrant epidermal growth factor receptor signaling and enhanced sensitivity to EGFR inhibitors in lung cancer. Cancer Res 2005;65:226–35.
32. Greulich H, Chen TH, Feng W, et al. Oncogenic transformation by inhibitor-sensitive and -resistant EGFR mutants. PLoS Med 2005;2:1167–76.
33. Yonesaka K, Tamura K, Kurata T, et al. Small interfering RNA targeting survivin sensitizes lung cancer cell with mutant p53 to Adriamycin. Int J Cancer 2006; 118:812–20.
34. Koizumi F, Shimoyama T, Taguchi F, Saijo N, Nishio K. Establishment of a human non-small cell lung cancer cell line resistant to gefitinib. Int J Cancer 2005;116:36–44.
35. Arteaga CL, Ramsey TT, Shawver LK, Guyer CA. Unliganded epidermal growth factor receptor dimerization induced by direct interaction of quinazolines with the ATP binding site. J Biol Chem 1997;272:23247–54.
36. Mukohara T, Engelman JA, Hanna NH, et al. Differential effects of gefitinib and cetuximab on non-small-cell lung cancers bearing epidermal growth factor receptor mutations. J Natl Cancer Inst 2005;97:1185–94.
37. Janmaat ML, Rodriguez JA, Gallegos-Ruiz M, Kruyt FA, Giaccone G. Enhanced cytotoxicity induced by gefitinib and specific inhibitors of the Ras or phosphatidyl inositol-3 kinase pathways in non-small cell lung cancer cells. Int J Cancer 2006;118:209–14.
38. Pao W, Miller VA, Politi KA, et al. Acquired resistance of lung adenocarcinomas to gefitinib or erlotinib is associated with a second mutation in the EGFR kinase domain. PLoS Med 2005;2:225–35.
39. Kobayashi S, Ji H, Yuza Y, et al. An alternative inhibitor overcomes resistance caused by a mutation of the epidermal growth factor receptor. Cancer Res 2005; 65:7096–101.
40. Olayioye MA, Neve RM, Lane HA, Hynes NE. The ErbB signaling network: receptor heterodimerization in development and cancer. EMBO J 2000;19:3159–67.
41. Okabayashi Y, Kid Y, Okutani T, Sugimoto Y, Sakaguchi K, Kasuga M. Tyrosines 1148 and 1173 of activated human epidermal growth factor receptors are binding sites of Shc in intact cells. J Biol Chem 1994;269: 18674–8.
42. Riemenschneider MJ, Bell DW, Haber DA, Louis DN. Pulmonary adenocarcinomas with mutant epidermal growth factor receptors. N Engl J Med 2005;352:1724–5.
43. Shigematsu H, Lin L, Takahashi T, et al. Clinical and biological features associated with epidermal growth factor receptor gene mutations in lung cancers. J Natl Cancer Inst 2005;97:339–46.
44. Calvo E, Baselga J. Ethnic differences in response to epidermal growth factor receptor tyrosine kinase inhibitors. J Clin Oncol 2006;24:2158–63.
45. Sugio K, Uramoto H, Ono K, et al. Mutations within the tyrosine kinase domain of EGFR gene specifically occur in lung adenocarcinoma patients with a low exposure of tobacco smoking. Br J Cancer 2006;94:896–903.
46. Riely GJ, Pao W, Pham D, et al. Clinical course of patients with non-small cell lung cancer and epidermal growth factor receptor exon 19 and exon 21 mutations treated with gefitinib or erlotinib. Clin Cancer Res 2006; 12:839–44.
47. Jackman DM, Yeap BY, Sequist LV, et al. Exon 19 deletion mutations of epidermal growth factor receptor are associated with prolonged survival in non-small cell lung cancer patients treated with gefitinib or erlotinib. Clin Cancer Res 2006;12:3908–14.

Association of Breast Cancer Stem Cells Identified by Aldehyde Dehydrogenase 1 Expression with Resistance to Sequential Paclitaxel and Epirubicin-Based Chemotherapy for Breast Cancers

Tomonori Tanei, Koji Morimoto, Kenzo Shimazu, Seung Jin Kim, Yoshio Tanji, Tetsuya Taguchi, Yasuhiro Tamaki, and Shinzaburo Noguchi

Abstract

Purpose: Breast cancer stem cells have been shown to be associated with resistance to chemotherapy *in vitro*, but their clinical significance remains to be clarified. The aim of this study was to investigate whether cancer stem cells were clinically significant for resistance to chemotherapy in human breast cancers.

Experimental Design: Primary breast cancer patients ($n = 108$) treated with neoadjuvant chemotherapy consisting of sequential paclitaxel and epirubicin-based chemotherapy were included in the study. Breast cancer stem cells were identified by immunohistochemical staining of CD44/CD24 and aldehyde dehydrogenase 1 (ALDH1) in tumor tissues obtained before and after neoadjuvant chemotherapy. $CD44^+/CD24^-$ tumor cells or ALDH1-positive tumor cells were considered stem cells.

Results: Thirty (27.8%) patients achieved pathologic complete response (pCR). ALDH1-positive tumors were significantly associated with a low pCR rate (9.5% versus 32.2%; $P = 0.037$), but there was no significant association between $CD44^+/CD24^-$ tumor cell proportions and pCR rates. Changes in the proportion of $CD44^+/CD24^-$ or ALDH1-positive tumor cells before and after neoadjuvant chemotherapy were studied in 78 patients who did not achieve pCR. The proportion of ALDH1-positive tumor cells increased significantly ($P < 0.001$) after neoadjuvant chemotherapy, but that of $CD44^+/CD24^-$ tumor cells did not.

Conclusions: Our findings suggest that breast cancer stem cells identified as ALDH1-positive, but not $CD44^+/CD24^-$, play a significant role in resistance to chemotherapy. ALDH1-positive thus seems to be a more significantly predictive marker than $CD44^+/CD24^-$ for the identification of breast cancer stem cells in terms of resistance to chemotherapy.

Cancer stem cells are defined as rare tumor cells that are capable of self-renewal and give rise to multipotent progenitor cells, which ultimately differentiate into all cell types within the tumor (1–4). The cancer stem cell population is believed to be small, accounting for only 0.1% to 1% of all tumor cells. Cancer stem cells were first documented in acute myeloid leukemia by taking advantage of cell sorting technology using various surface markers (5). Later studies of solid tumors, including breast tumors, brain tumors, lung tumors, and colon tumors, have indicated the presence of cancer stem cells in these tumors as well (6–9). With respect to breast cancer, Al-Hajj et al. were the first to distinguish tumorigenic cancer cells (stem cells) from nontumorigenic ones by using cell surface markers CD44 and CD24 (6). They showed that as few as 100 tumor cells with $CD44^+/CD24^-$ phenotype were able to produce tumors in immunodeficient mice, whereas tumor cells with other CD44/CD24 phenotypes were unable or rarely able to produce tumors even when as many as 10^5 to 10^6 tumor cells were inoculated into such mice. Furthermore, Abraham et al. conducted immunohistochemical studies of $CD44^+/CD24^-$ tumor cells in human breast tumors and showed that breast tumors containing a high proportion of $CD44^+/CD24^-$ cells were associated with distant metastases (10).

Recently, Ginestier et al. showed that aldehyde dehydrogenase 1 (ALDH1) is a better marker of breast cancer stem cells based on the finding that fewer ALDH1-positive than

Authors' Affiliation: Department of Breast and Endocrine Surgery, Osaka University Graduate School of Medicine, Osaka, Japan

Received 6/12/08; revised 2/5/09; accepted 3/15/09; published OnlineFirst 6/9/09.

Grant support: Scientific Research on Priority Areas from the Ministry of Education, Culture, Sports, Science and Technology, Japan and Promotion of Cancer Research (Japan) for the Third-Term Comprehensive 10-Year Strategy for Cancer Control.

The costs of publication of this article were defrayed in part by the payment of page charges. This article must therefore be hereby marked *advertisement* in accordance with 18 U.S.C. Section 1734 solely to indicate this fact.

Note: Supplementary data for this article are available at Clinical Cancer Research Online (http://clincancerres.aacrjournals.org/).

Requests for reprints: Shinzaburo Noguchi, Department of Breast and Endocrine Surgery, Osaka University Graduate School of Medicine, 2-2 Yamadaoka, Suita-shi, Osaka 565-0871, Japan. Phone: 81-6-6879-3772; Fax: 81-6-6879-3779; E-mail: noguchi@onsurg.med.osaka-u.ac.jp.

doi:10.1158/1078-0432.CCR-08-1479

Translational Relevance

To realize the personalized chemotherapy for breast cancer patients, it is very important to develop a predictor of response to chemotherapy. Several parameters, including estrogen receptor, progesterone receptor, HER-2, Ki-67, and topoisomerase 2A, have been reported to be associated with pathologic complete response rates after sequential taxane and anthracycline-based chemotherapy, but they are not enough, and more accurate predictors need to be developed. In the present study, we have evaluated the clinical value of aldehyde dehydrogenase 1 (ALDH1)-positive cancer stem cells determined by immunohistochemistry in the prediction of response to the chemotherapy, because cancer stem cells are thought to be inherently chemoresistant and thus to have a potential to be used as a predictor of resistance. Actually, we have been able to show herein that ALDH1-positive cancer stem cells serve as a significant and independent predictor of resistance to the chemotherapy. Our present observation seems to be clinically important, because it is expected that response to sequential taxane and anthracycline-based chemotherapy can be estimated more accurately by adding ALDH1 to other conventional parameters.

$CD44^+/CD24^-$ tumor cells are required to produce tumors in immunodeficient mice (11). In addition, they have been able to show that immunohistochemically identified ALDH1 expression is associated with poor prognosis in human breast cancers. ALDH1 in cancer stem cells may be a significant enzyme in stem cell differentiation that regulates the conversion of retinoic acid to oxidizing retinol (12). The results of Abraham et al. (10) and Ginestier et al. (11) seem to point to the existence of breast cancer stem cells and their association with a biologically aggressive phenotype. Another important characteristic of cancer stem cells is that they usually express high levels of ATP-binding cassette transporters and thus are thought to be resistant to various chemotherapeutic agents effluxed by ATP-binding cassette transporters (13, 14). In fact, several *in vitro* studies have shown that cancer stem cells are resistant to paclitaxel, doxorubicin, 5-fluorouracil, and platinum (15–18). The implication that breast tumors may contain stem cells, which are supposedly resistant to chemotherapy, can be of major clinical importance for a better understanding of the mechanism of acquisition of drug resistance. Almost all breast tumors, although initially may respond to a given chemotherapy, ultimately become resistant to the chemotherapy. It is generally thought that tumor regrowth during chemotherapy results from clonal selection of tumor cells, which acquire their resistant properties due to various genetic/epigenetic mechanisms during the treatment (2). In the case of stem cells, however, it is considered that chemotherapy-resistant stem cells have been already present before chemotherapy and that tumor regrowth is attributable to the preferential proliferation of these stem cells. Taking all these findings into account leads to the speculation that breast tumors with a high proportion of stem cells may be associated with resistance to chemotherapy and that the proportion of stem cells may increase after chemotherapy because they are resistant to chemotherapy. In the study presented here, we investigated the validity of these speculations in a neoadjuvant chemotherapy setting in human breast cancers. We employed the two methods for the identification of breast cancer stem cells, CD44/CD24 and ALDH1, to compare their clinical utility for the prediction of resistance to chemotherapy.

Materials and Methods

Patients and breast tumor tissues. The subjects recruited for this study comprised 108 primary invasive breast cancer patients (mean age, 50.8 years; range, 26-72 years) with a tumor >3 cm in diameter or with cytologically confirmed axillary lymph node involvement who were treated with neoadjuvant chemotherapy at Osaka University Hospital between June 2003 and April 2007 (4 stage IV patients with small distant metastases were included in these subjects). Tumor specimens were obtained before neoadjuvant chemotherapy by means of vacuum-assisted core needle biopsy. All patients were treated with 12 cycles of paclitaxel (80 mg/m^2/wk) followed by 4 cycles of 5-fluorouracil 500 mg/m^2, epirubicin 75 mg/m^2, and cyclophosphamide 500 mg/m^2 every 3 weeks. Breast conserving surgery or mastectomy was conducted 3 to 4 weeks after the last treatment. Tumor specimens (surgical specimens) were also obtained at surgery. Informed consent was obtained from each patient.

It was possible that different sampling methods of tissue specimens might bias against the immunohistochemical results. Thus, we conducted a study to compare the immunohistochemical results of CD44/CD24 and ALDH1 between the vacuum-assisted core needle biopsy specimens obtained before surgery and the surgical specimens obtained at surgery in 40 primary invasive breast cancer patients [stage I (n = 24), stage II (n = 15), and stage III (n = 1)] who had not been treated with neoadjuvant chemotherapy. Concordance of $CD44^+/CD24^-$ tumor cell proportions (%) as well as ALDH1 status between vacuum-assisted core needle biopsy and surgical specimens was excellent, indicating that difference in sampling methods of tissue specimens was unlikely to bias against our results (Supplementary Fig. S1).

Antibodies. (*a*) CD24 [clone Ab-1 (SN3), monoclonal, IgG isotype, 1:100; Neomarkers], (*b*) Tyramide Signal Amplification Fluorescence System (1:50; Perkin-Elmer), (*c*) biotin-conjugated CD44 (clone 156-3C11, monoclonal, IgG isotype, 1:100; Neomarkers), (*d*) ALDH1 (monoclonal, IgG isotype, 1:100; BD Biosciences), (*e*) CD68 (clone PG-M1, monoclonal, IgG isotype, 1:100; DAKO Japan), (*f*) Ki-67 (clone MIB-1, monoclonal, IgG isotype, 1:100; DAKO Japan), (*g*) topoisomerase 2A (TOP2A; clone Ki-S1, monoclonal, IgG isotype, 1:100; DAKO Japan), (*h*) biotin Labeling Kit-NH_2 (Dojindo Molecular Technologies), and (*i*) Tyramide Signal Amplification Biotin System (1:50, Perkin-Elmer).

Double-fluorescence immunohistochemical identification of CD44+/CD24- tumor cells. Antigen retrieval of tumor tissue paraffin sections (3 μm) was accomplished by microwaving in Target Retrieval Solution (pH 6.0; DAKO Japan). The sections were first incubated with anti-CD24 antibody (*a*) and then anti-mouse secondary antibody conjugated with peroxidase (1:100; The Jackson Laboratory) and subsequently visualized with a FITC-Tyramide Signal Amplification reaction (*b*; ref. 19). Next, the paraffin sections were incubated with anti-biotin-conjugated CD44 antibody (*c*) and subsequently visualized by means of anti-biotin secondary antibody conjugated with Cy3 (1:100; The Jackson Laboratory) and then counterstained with Hoechst (Invitrogen).

Fluorescent immunostaining of CD44 and CD24 was analyzed with a Zeiss LSM510 confocal microscope. The percentage of $CD44^+/CD24^-$ tumor cells (stained red) was determined with the aid of WinROOF imaging software (Mitani; ref. 20). $CD44^+/CD24^-$ tumor cells were selected by subtracting $CD24^+$ tumor cells from $CD44^+$ tumor cells. The number of $CD44^+/CD24^-$ tumor cells and the other tumor cells in the invasive

component was counted with visual check [three high-power (×400) fields]. Finally, the percentage of $CD44^+/CD24^-$ tumor cells per total tumor cells was calculated in each tumor. Threshold values used for the analysis of CD44 (Cy3) and CD24 (FITC) images were 33.3% (85 on the 0-255 grayscale) and 20.0% (51 on the 0-255 grayscale), respectively.

Immunohistochemical staining of ALDH1, CD68, Ki-67, and TOP2A. The expression of ALDH1, CD68, Ki-67, and TOP2A was immunohistochemically evaluated with the avidin-biotin-peroxidase method using anti-ALDH1 antibody (*d*), anti-CD68 antibody (*e*), anti-Ki-67 antibody (*f*), and anti-TOP2A antibody (*g*), respectively, according to the previously described method (21, 22). Antigen retrieval was accomplished by heating at 98°C for 40 min for ALDH1, CD68, and Ki-67 and for 1 h for TOP2A. The cutoff value for Ki-67 and TOP2A was 20%.

For differentiation of ALDH1-positive tumor cells from ALDH1-positive macrophages, double immunohistochemical staining of ALDH1 and CD68 (a marker for macrophages) were carried out in some tumors. In brief, paraffin sections (3 μm) were incubated with anti-ALDH1 antibody (*d*) and subsequent conjugation of anti-mouse secondary antibody with alkaline phosphatase. Then, the sections were incubated with anti-CD68 antibody (*e*), treated with Biotin Labeling Kit-NH_2 (*h*), and incubated with anti-biotin secondary antibody conjugated with peroxidase using Tyramide Signal Amplification Biotin System (*i*; ref. 23). Finally, the sections were incubated with fucshin (DAKO Japan) and 3,3′-diaminobenzidine (Merck). Incubation with primary antibodies were done at 4°C for overnight and that with secondary antibodies were done at room temperature for 1 h.

Histologic grade, estrogen receptor, progesterone receptor, and HER-2. The histologic grade was determined with the Scarff-Bloom-Richardson grading system (24). Estrogen receptor (ER) and progesterone receptor (PR) were defined as positive, when ≥10% of the tumor cells were immunohistochemically stained positive (ER: clone 6F11; PR: clone 16; Ventana Japan and SRL). HER-2 was determined by fluorescence *in situ* hybridization using PathVysion HER-2 DNA Probe kits (SRL). When a tumor contained more than two genes per cell, it was considered HER-2 positive.

Assessment of pathologic response. Pathologic response of breast cancers to neoadjuvant chemotherapy was assessed for all patients. Multiple slides prepared from the primary tumors were examined for evaluation of chemotherapeutic effect according to the criteria specified in the General Rules for Clinical and Pathological Recording of Breast Cancer 2005 (25). In this study, pathologic complete response (pCR) was defined as the absence of residual invasive components regardless of the presence or absence of ductal carcinoma *in situ* components.

Colony formation assay. Colony formation assay of breast tumor cells was carried out to investigate the relationship of $CD44^+/CD24^-$ or ALDH1 positive with colony formation ability in 27 primary invasive breast cancers [stage 1 ($n = 2$), stage 2 ($n = 23$), and stage 3 ($n = 2$)] who had not been treated with neoadjuvant chemotherapy using the collagen gel droplet-embedded culture-drug sensitivity test kits (Nitta Gelatin; refs. 26–28). ALDH1-positive tumors showed a significantly ($P = 0.046$) higher colony formation than ALDH1-negative tumors, although there was no significant difference in colony formation between $CD44^+/CD24^-$ high and low tumors (Supplementary Fig. S2).

Statistical analyses. The SPSS software package version 12.1 was used for all statistical analyses. Association of the immunohistochemical results of CD44/CD24 and ALDH1 with the various clinicopathologic parameters were evaluated by the Mann-Whitney *U* test or χ^2 test. Changes in the immunohistochemical results of CD44/CD24 and ALDH1 before and after neoadjuvant chemotherapy were assessed by the Wilcoxon signed-rank test and χ^2 test, respectively. The relationship between pCR rates and various parameters was evaluated using a logistic regression method. Statistical significance was assumed for $P < 0.05$.

Results

Double-fluorescence immunohistochemical staining of CD44 and CD24. We analyzed $CD44^+/CD24^-$ tumor cells in human breast cancer tissues by the double-fluorescence immunohistochemical staining method. Representative results are shown in Fig. 1A (CD44), Fig. 1B (CD24), and Fig. 1C (CD44/CD24). $CD44^+$ tumor cells and $CD24^+$ tumor cells were selected by WinROOF imaging software (Fig. 1D and E, respectively), and $CD44^+/CD24^-$ tumor cells (Fig. 1F) were determined by subtracting $CD24^+$ cells (Fig. 1E) from $CD44^+$ cells (Fig. 1D). Finally, $CD44^+/CD24^-$ tumor cell proportion (%) was calculated in each tumor.

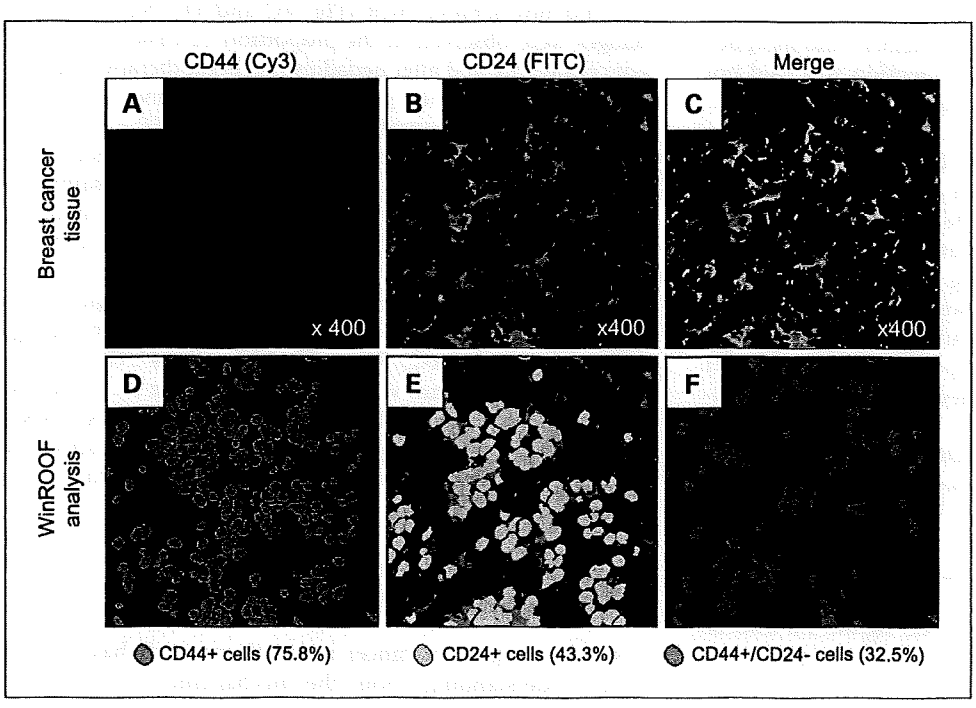

Fig. 1. Double-fluorescence immunohistochemical identification of $CD44^+/CD24^-$ tumor cells. Breast cancer tissue were subjected to double-fluorescence immunohistochemical determination of $CD44^+/CD24^-$ tumor cells. $CD44^+$ tumor cells were stained red (*A*) and $CD24^+$ tumor cells were stained green (*B*). Pictures *A* and *B* were merged into picture *C*. For the calculation of $CD44^+/CD24^-$ tumor cell proportions in breast cancer tissues, $CD44^+$ tumor cells and $CD24^+$ tumor cells were selected by WinROOF imaging software. $CD44^+$ tumor cells were shown in pink (*D*), accounting for 75.8% of all tumor cells, and $CD24^+$ tumor cells were shown in light blue (*E*), accounting for 43.3% of all tumor cells. Proportion (32.5%) of $CD44^+/CD24^-$ tumor cells (*F*) in all tumor cells was then determined by subtracting $CD24^+$ cells (*E*) from $CD44^+$ cells (*D*).

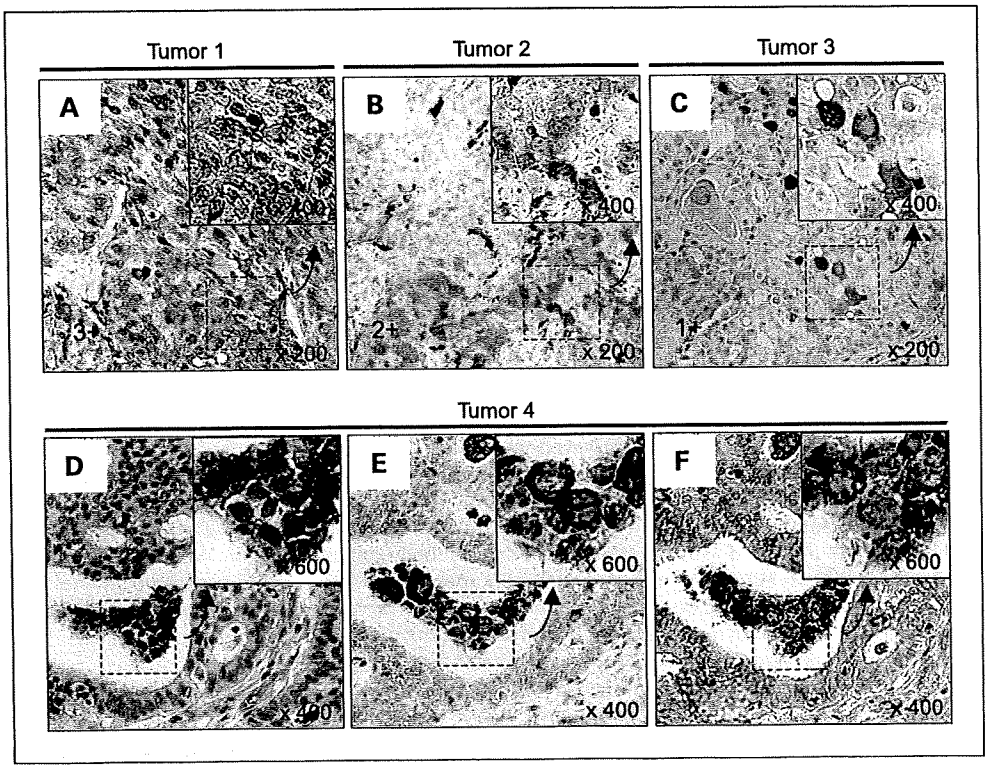

Fig. 2. Immunohistochemical identification of ALDH1-positive tumor cells. Representative results of immunostaining of ALDH1 in breast cancer tissues: (*A*) 3+ in tumor 1, (*B*) 2+ in tumor 2, and (*C*) 1+ in tumor 3. In tumor 4, besides ALDH1 immunostaining (fuchsin: *red*; *D*), CD68 immunostaining (3,3'-diaminobenzidine: *brown*; *E*) as well as ALDH1 and CD68 double immunostaining (*F*) were done in the adjacent sections.

Immunohistochemical staining of ALDH1. Representative results of immunohistochemical staining of ALDH1 in human breast cancer tissues were shown in Fig. 2. By using the criteria described by the report of Ginestier et al. (11), immunohistochemical staining of ALDH1 was classified into 3+ (≥50% positive tumor cells), 2+ (<50%, ≥10%), 1+ (<10%, ≥5%), and negative (<5%) groups. For the subsequent analysis, tumors showing 1+, 2+, and 3+ expression of ALDH1 were considered to be ALDH1 positive.

Because macrophages were positive for ALDH1 and morphologically similar to tumor cells, special attention was paid not to misinterpret macrophages as tumor cells positive for ALDH1. For this reason, in some tumors where differentiation between ALDH1-positive tumor cells and ALDH1-positive macrophages was difficult, immunostaining of CD68 as well as double staining of ALDH1 (fuchsin: red) and CD68 (3,3'-diaminobenzidine: brown) was done for the adjacent sections. Results for a representative tumor were shown in Fig. 2. In tumor 4 in Fig. 2, tumor-like cells in the ductal lumen were positive for ALDH1 (Fig. 2D) but also for CD68 (Fig. 2E), and double staining confirmed that these tumor-like cells were positive for both ALDH1 and CD68 (Fig. 2F), indicating that they were actually ALDH1-positive macrophages.

Relationship of CD44+/CD24- or ALDH1 positive with clinicopathologic features of breast tumors as well as response to neoadjuvant chemotherapy. As shown in Table 1, there was no significant association of $CD44^+/CD24^-$ tumor cell proportions or of ALDH1-positive tumors with various clinicopathologic features such as menopausal status, tumor size, histologic grade, ER, PR, or HER-2. There was also no significant association between $CD44^+/CD24^-$ tumor cell proportions and ALDH1 status (Fig. 3B).

The pCR was achieved by 30 (27.8%) of the 108 patients treated with neoadjuvant chemotherapy. ALDH1-positive tumors were significantly associated with low pCR rates (P = 0.037; Fig. 4B), but there was no significant association between $CD44^+/CD24^-$ tumor cell proportions and pCR rates (Fig. 4A). Changes in the proportions of $CD44^+/CD24^-$ tumor cells or in grading of ALDH1-positive tumor cells before and after neoadjuvant chemotherapy were examined in 78 patients who did not achieve pCR (Fig. 4C and D). No significant changes were observed in the proportion of $CD44^+/CD24^-$ tumor cells before and after neoadjuvant chemotherapy (Fig. 4C). On the other hand, the grade of ALDH1-positive tumor cells after neoadjuvant chemotherapy significantly ($P < 0.001$) increased (Fig. 4D) in 9 patients (3 from 0 to 1+, 2 from 1+ to 2+, 2 from 1+ to 3+, and 2 from 2+ to 3+). A representative case where ALDH1 expression increased from 1+ before neoadjuvant chemotherapy (Fig. 4D, *a*) to 2+ after neoadjuvant chemotherapy (Fig. 4D, *b*) was shown.

Relationship between various biological factors and pCR rates. Association of various biological factors such as histologic grade, ER, PR, HER-2, Ki-67, TOP2A, $CD44^+/CD24^-$, and ALDH1 with pCR rates was also studied (Table 2). Univariate analysis showed a significant association of ER, PR, HER-2, Ki-67, TOP2A, and ALDH1 with pCR rates, and multivariate analysis showed a significant association of ER, Ki-67, and ALDH1 with pCR rates.

Discussion

Recent progress in cancer stem cell research has led to a better understanding about the mechanism of resistance to

chemotherapy as well as to the development of more effective chemotherapeutic regimens and new antitumor agents (29). Although their number is very small, cancer stem cells are thought to be inherently drug resistant, so that their eradication is essential for long-term success in cancer treatment (30, 31). An association between cancer stem cells and drug resistance in breast cancer cell lines has been shown *in vitro* (15–17), but such an association has not been shown yet clinically in human breast cancers. In the current study, we therefore investigated whether stem cells are associated with drug resistance in breast cancer patients treated with neoadjuvant chemotherapy.

Al-Hajj et al. have shown that $CD44^+/CD24^-$ tumor cells were highly tumorigenic in immunodeficient mice and that cancer stem cells in this population appeared to be enriched (6). It therefore seemed to be of considerable interest to identify the clinicopathologic characteristics of breast cancers with a high proportion of $CD44^+CD24^-$ tumor cells. We studied breast cancer tissues with the double-fluorescence immunohistochemistry and found that $CD44^+/CD24^-$ tumor cell proportions were not significantly associated with the conventional clinicopathologic features such as menopausal status, tumor size, lymph node status, histologic grade, ER, PR, or HER-2, which was also consistent with previously reported results (10).

Because cancer stem cells are thought to be inherently resistant to chemotherapy, $CD44^+/CD24^-$ high tumors can be expected to show a greater resistance to neoadjuvant chemotherapy than $CD44^+/CD24^-$ low tumors. Our study, however, has shown that there is no significant association between $CD44^+/CD24^-$ tumor cell proportions and pCR rates. Besides, $CD44^+/CD24^-$ tumor cell proportions have not shown a significant increase after neoadjuvant chemotherapy, although chemotherapy-resistant stem cells are expected to increase. These results seem to suggest that stem cells identified by immunohistochemistry of $CD44^+/CD24^-$ may not play an important role in the resistance to chemotherapy in human breast cancer. However,

Table 1. Relationship of $CD44^+/CD24^-$ tumor cell proportions (%) or ALDH1-positive tumors with clinicopathologic parameters

	n	$CD44^+/CD24^-$ cell population (%)		ALDH1		
		Median (IQR)*	$P^\dagger$	Positive, *n* (%)	Negative, *n* (%)	$P^\ddagger$
All breast carcinomas	108			21 (19)	87 (81)	
Histologic type			0.020			0.360
Invasive lobular cancer	11	10.4 (0.0-17.3)		1 (9)	10 (91)	
Invasive ductal cancer	97	23.8 (10.4-35.3)		20 (21)	77 (79)	
Histologic grade						0.151
1	11	24.5 (12.4-38.1)		0 (0)	11 (100)	
2	76	22.4 (10.3-35.3)	0.878	15 (20)	61 (80)	
3	21	18.4 (8.2-29.7)	0.292	6 (29)	15 (71)	
Tumor size (cm)						0.145
T_1	6	23.8 (4.0-26.8)		1 (17)	5 (83)	
T_2	59	25.3 (10.3-42.0)	0.496	7 (12)	52 (88)	
T_3	30	18.1 (4.7-24.8)	0.470	9 (30)	21 (70)	
T_4	13	23.8 (10.1-35.3)	1.000	4 (31)	9 (69)	
Lymph node metastasis			0.276			0.124
N (-)	30	24.5 (14.5-35.2)		3 (10)	27 (90)	
N (+)	78	20.5 (7.2-35.3)		18 (23)	60 (77)	
ER			0.120			0.184
-	38	25.2 (16.1-36.5)		10 (26)	28 (74)	
+	70	19.7 (4.7-34.9)		11 (16)	59 (84)	
PR			0.610			0.797
-	59	21.7 (12.8-35.2)		12 (20)	47 (80)	
+	49	21.1 (7.2-35.2)		9 (18)	40 (82)	
HER-2			0.253			0.548
-	82	23.8 (9.5-36.5)		17 (21)	65 (79)	
+	26	19.2 (8.4-25.1)		4 (15)	22 (85)	
Ki-67			0.295			0.148
<20%	62	22.4 (10.3-35.3)		9 (15)	53 (85)	
≥20%	46	22.4 (10.3-35.3)		12 (26)	34 (74)	
TOP2A			0.037			0.029
<20%	59	21.1 (4.4-30.7)		7 (12)	52 (88)	
≥20%	49	25.3 (14.0-39.9)		14 (29)	35 (71)	
Stage						0.090
II	59	26.4 (14.8-42.0)		7 (12)	52 (88)	
III	45	17.7 (4.7-24.8)	0.002	13 (29)	32 (71)	
IV	4	9.6 (0.0-29.8)	0.142	1 (25)	3 (75)	

*IQR, interquartile range (25%, 75%).
†Mann-Whitney *U* test.
‡χ^2 test.

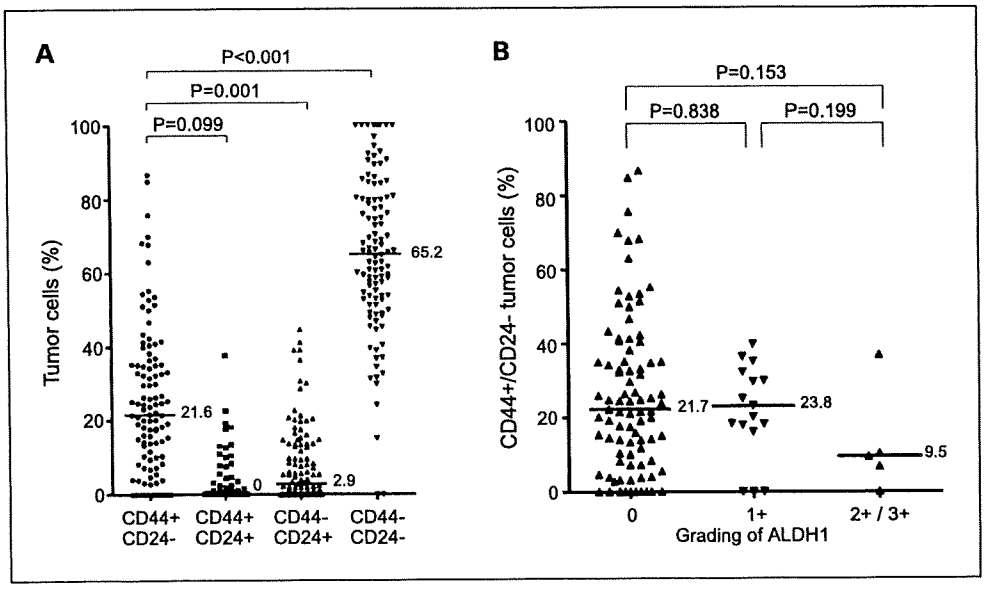

Fig. 3. Proportions of $CD44^+/CD24^+$ tumor cells in each tumor and their relationship with ALDH1 status. Breast cancers ($n = 108$) were classified into the four categories: $CD44^+/CD24^-$, $CD44^+/CD24^+$, $CD44^-/CD24^+$, and $CD44^-/CD24^-$. Proportions (%) of tumor cells in each category were plotted for each tumor (*A*). Breast cancers ($n = 108$) were graded by ALDH1 staining (0, 1+, 2+, and 3+), and their relationship with $CD44^+/CD24^-$ tumor cell proportions (%) was shown (*B*). *P*, Mann-Whitney *U* test. *Bars*, median.

Li et al. recently reported that neoadjuvant chemotherapy increased the proportions of $CD44^+/CD24^-$ tumor cells identified by flow cytometry (32). The reason for this discrepancy has been currently unknown, but it might be, at least in part, explained by the difference in the method for determination of $CD44^+/CD24^-$ tumor cells, that is, immunohistochemical double staining versus flow cytometry as well as the difference in the regimens and duration of neoadjuvant chemotherapy (paclitaxel followed by 5-fluorouracil 500 mg/m^2, epirubicin 75 mg/m^2, and cyclophosphamide 500 mg/m^2 every 3 weeks for 24 weeks versus docetaxel or doxorubicin/cyclophosphamide for 12 weeks).

Very recently, it was reported by Ginestier et al. that ALDH1 could function as a better marker of breast cancer stem cells than $CD44^+/CD24^-$ (11). We therefore also tried to clarify the clinicopathologic characteristics of ALDH1-positive breast tumors but found that ALDH1 expression was not significantly associated with any conventional clinicopathologic features. On the other hand, a significant association was found between ALDH1-positive breast tumors and resistance to neoadjuvant chemotherapy, because pCR rates were significantly lower in ALDH1-positive tumors (9.5%) than ALDH1-negative tumors (32.2%). In addition, a significant increase in the proportion of ALDH1-positive tumor cells was observed after neoadjuvant chemotherapy. These results seem to indicate that ALDH1-positive tumor cells play a significant role in resistance to chemotherapy. Because Ginestier et al. have reported that ALDH1 tumor cells are more tumorigenic than $CD44^+/CD24^-$ tumor cells (11), breast cancer stem cells are thought to be richer in ALDH1-positive tumor cells than in $CD44^+/CD24^-$ tumor cells. Consistently, we have also been able to show that ALDH1 positive, but not $CD44^+/CD24^-$, is significantly associated with colony formation in the collagen gel.

It has been reported that the subset of ALDH1-positive and $CD44^+/CD24^-$ tumor cells contain the highest proportion of breast cancer stem cells (11); thus, this subset is speculated to be most resistant to chemotherapy. However, our present study has shown that pCR rates in the ALDH1-positive and $CD44^+/CD24^-$ high subset (20%, 2 of 10) are not lowest among all the subsets, that is, the ALDH1-positive and $CD44^+/CD24^-$ low subset (0%, 0 of 11), the ALDH1-negative and $CD44^+/CD24^-$ high subset (34.1%, 15 of 44), and the ALDH1-negative and $CD44^+/CD24^-$ low subset (30.2%, 13 of 43). Addition of CD44/CD24 status to ALDH1 status seems not to improve the prediction of response to chemotherapy. These findings taken together lead us to consider that ALDH1-positive tumor cells are likely to serve as a better marker for breast cancer stem cells than $CD44^+/CD24^-$ tumor cells at least for the prediction of resistance to chemotherapy. We speculate that ALDH1-positive tumors are resistant to chemotherapy, because such tumors contain a higher proportion of cancer stem cells. It is also possible, however, that ALDH1-positive tumor cells, irrespective of whether they are cancer stem cells or not, might be involved in resistance to chemotherapy, because ALDH1 itself has been shown to play a significant role in the resistance to chemotherapy in hematopoietic cells (33). Development of a highly specific marker for breast cancer stem cells, as well as further clarification of a role of ALDH1 in resistance to chemotherapy in breast cancers, is needed to elucidate a genuine role of breast cancer stem cells in resistance to chemotherapy.

Several biological factors, including ER, PR, HER-2, Ki-67, and TOP2A, have been reported to be associated with pCR rates after sequential taxane and anthracycline-based chemotherapy (34–38). In our study, we were able to obtain results consistent with previously reported ones in that high pCR rates were associated with negative ER, negative PR, positive HER-2, high Ki-67, and high TOP2A. Interestingly, multivariate analysis including these factors as well as ALDH1 has shown that three factors, ER, Ki-67, and ALDH1, are significant and mutually independent predictors of response to chemotherapy. We therefore believe that response to sequential paclitaxel and epirubicin-based chemotherapy can be estimated more accurately by adding ALDH1 to ER and Ki-67. The clinical significance of identification of these three markers for the prediction of response to sequential taxane and anthracycline-based chemotherapy therefore seems to deserve further investigation.

In conclusion, we were able to show that ALDH1 positive, but not $CD44^+/CD24^-$, was significantly associated with

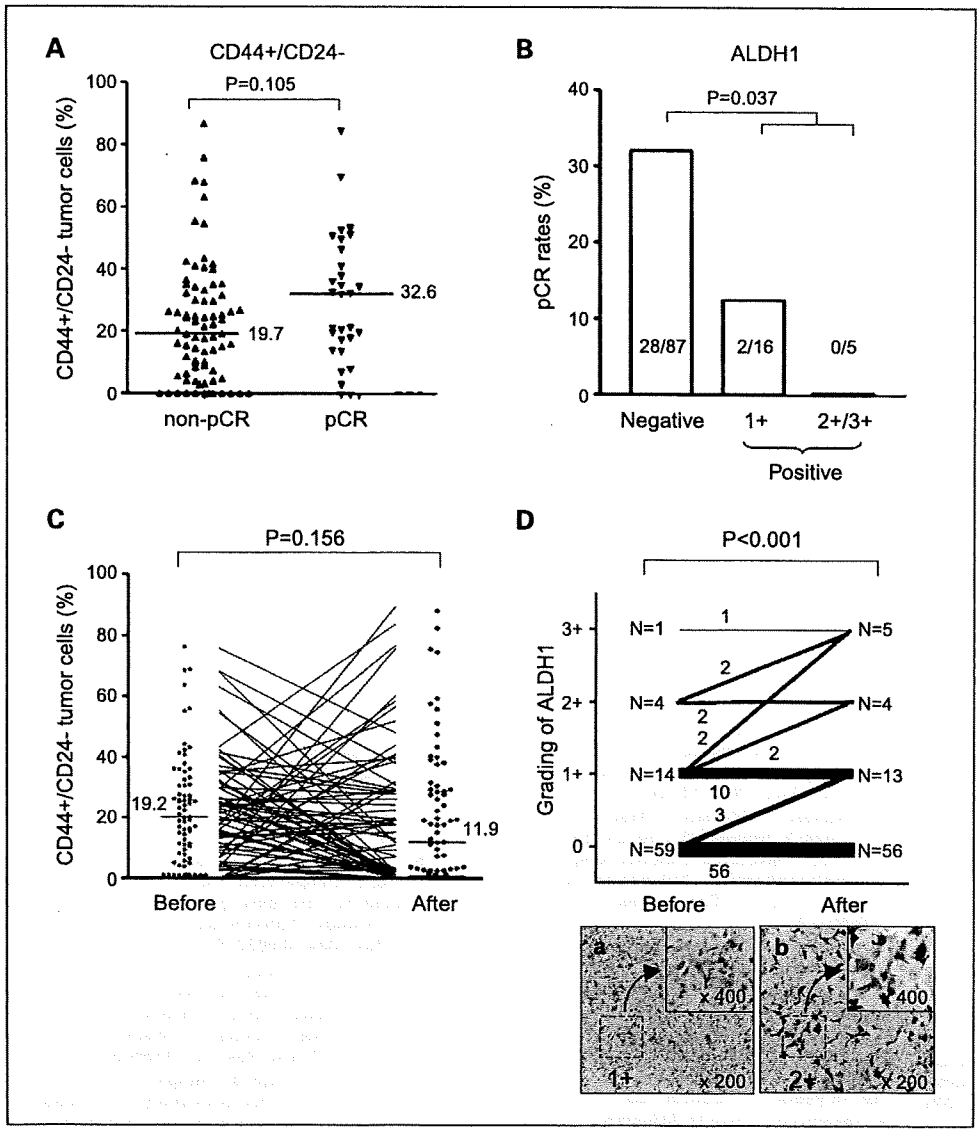

Fig. 4. Relationship of $CD44^+/CD24^-$ or ALDH1 positive with response to neoadjuvant chemotherapy. $CD44^+/CD24^-$ tumor cell proportions (%) were compared between tumors with pCR and non-pCR (*A*). *P*, Mann-Whitney *U* test. *Bars*, median. pCR rates were compared between ALDH1-positive and ALDH1-negative tumors (*B*). *P*, χ^2 test. Proportions of $CD44^+/CD24^-$ tumor cells (*C*) and ALDH1-positive tumor cells (*D*) were compared before and after neoadjuvant chemotherapy in 78 tumors not achieving pCR. *P*, Wilcoxon signed-rank test. Representative results of immunohistochemical staining of ALDH1 before (*D, a*) and after (*D, b*) neoadjuvant chemotherapy in the same patient, indicating up-regulation from ALDH1 1+ to 2+.

resistance to sequential paclitaxel and epirubicin-based chemotherapy and that the expression of ALDH1 increased after neoadjuvant chemotherapy, indicating that breast cancer stem cells identified by ALDH1 actually played a significant role in resistance to chemotherapy. This means that ALDH1 positive seems to be a better marker than $CD44^+/CD24^-$ for the identification of breast cancer stem cells at least for the prediction of resistance to chemotherapy. However,

Table 2. Univariate and multivariate analyses of various predictors of pCR

	pCR rate (%)	Univariate analysis		Multivariate analysis	
		Odds ratio	*P*	Odds ratio	*P*
Histologic grade (3/1, 2)	38.1/25.3	1.818	0.244		
ER (-/+)	50.0/15.7	5.362	<0.001	5.987	0.022
PR (-/+)	37.3/16.3	3.047	0.018	0.567	0.477
HER-2 (+/-)	46.1/22.0	3.048	0.019	2.479	0.114
Ki-67 (≥20% vs <20%)	45.7/14.5	4.944	<0.001	3.522	0.042
TOP2A (≥20% vs <20%)	38.8/18.6	2.763	0.022	1.329	0.638
ALDH1 (-/+)	32.2/9.5	4.508	0.037	8.584	0.011
$CD44^+/CD24^-$ (high/low)*	31.5/24.1	1.449	0.391		

*$CD44^+/CD24^-$ high and low tumors were determined using a median value (21.6%) as the cutoff value.

our observation needs to be confirmed by a future study including a larger number of patients and different chemotherapeutic regimens.

Disclosure of Potential Conflicts of Interest

No potential conflicts of interest were disclosed.

References

1. Ward RJ, Dirks PB. Cancer stem cells: at the headwaters of tumor development. Annu Rev Pathol 2007;2:175–89.
2. Reya T, Morrison SJ, Clarke MF, Weissman IL. Stem cells, cancer, and cancer stem cells. Nature 2001;414:105–11.
3. Molofsky AV, Pardal R, Morrison SJ. Diverse mechanisms regulate stem cell self-renewal. Curr Opin Cell Biol 2004;16:700–7.
4. Morrison SJ, Wandycz AM, Hemmati HD, Wright DE, Weissman IL. Identification of a lineage of multipotent hematopoietic progenitors. Development 1997;124:1929–39.
5. Lapidot T, Sirard C, Vormoor J, et al. A cell initiating human acute myeloid leukaemia after transplantation into SCID mice. Nature 1994; 367:645–8.
6. Al-Hajj M, Wicha MS, Benito-Hernandez A, Morrison SJ, Clarke MF. Prospective identification of tumorigenic breast cancer cells. Proc Natl Acad Sci U S A 2003;100:3983–8.
7. Singh SK, Hawkins C, Clarke ID, et al. Identification of human brain tumour initiating cells. Nature 2004;432:396–401.
8. Kim CF, Jackson EL, Woolfenden AE, et al. Identification of bronchioalveolar stem cells in normal lung and lung cancer. Cell 2005;121:823–35.
9. O'Brien CA, Pollett A, Gallinger S, Dick JE. A human colon cancer cell capable of initiating tumour growth in immunodeficient mice. Nature 2007;445:106–10.
10. Abraham BK, Fritz P, McClellan M, Hauptvogel P, Athelogou M, Brauch H. Prevalence of $CD44^{+}/CD24^{-/low}$ cells in breast cancer may not be associated with clinical outcome but may favor distant metastasis. Clin Cancer Res 2005;11:1154–9.
11. Ginestier C, Hur MH, Charafe-Jauffret E, et al. ALDH1 is a marker of normal and malignant human mammary stem cells and a predictor of poor clinical outcome. Cell Stem Cell 2007;1:555–67.
12. Chute JP, Muramoto GG, Whitesides J, et al. Inhibition of aldehyde dehydrogenase and retinoid signaling induces the expansion of human hematopoietic stem cells. Proc Natl Acad Sci U S A 2006; 103:11707–12.
13. Gillet JP, Efferth T, Remacle J. Chemotherapy-induced resistance by ATP-binding cassette transporter genes. Biochim Biophys Acta 2007; 1775:237–62.
14. Raaijmakers MH. ATP-binding-cassette transporters in hematopoietic stem cells and their utility as therapeutical targets in acute and chronic myeloid leukemia. Leukemia 2007;21: 2094–102.
15. Liu G, Yuan X, Zeng Z, et al. Analysis of gene expression and chemoresistance of $CD133^{+}$ cancer stem cells in glioblastoma. Mol Cancer 2006;5:67.
16. Ghods AJ, Irvin D, Liu G, et al. Spheres isolated from 9L gliosarcoma rat cell line possess chemoresistant and aggressive cancer stem-like cells. Stem Cells 2007;25:1645–53.
17. Fillmore CM, Kuperwasser C. Human breast cancer cell lines contain stem-like cells that self-renew, give rise to phenotypically diverse progeny and survive chemotherapy. Breast Cancer Res 2008;10:R25.
18. Haraguchi N, Utsunomiya T, Inoue H, et al. Characterization of a side population of cancer cells from human gastrointestinal system. Stem Cells 2006;24:506–13.
19. Wang G, Achim CL, Hamilton RL, Wiley CA, Soontornniyomkij V. Tyramide signal amplification method in multiple-label immunofluorescence confocal microscopy. Methods 1999; 18:459–64.
20. Hatanaka Y, Hashizume K, Nitta K, Kato T, Itoh I, Tani Y. Cytometrical image analysis for immunohistochemical hormone receptor status in breast carcinomas. Pathol Int 2003;53:693–9.
21. Miyoshi Y, Kurosumi M, Kurebayashi J, et al. Low nuclear grade but not cell proliferation predictive of pathological complete response to docetaxel in human breast cancers. J Cancer Res Clin Oncol 2008;134:561–7.
22. Takahashi Y, Miyoshi Y, Morimoto K, Taguchi T, Tamaki Y, Noguchi S. Low LATS2 mRNA level can predict favorable response to epirubicin plus cyclophosphamide, but not to docetaxel, in breast cancers. J Cancer Res Clin Oncol 2007; 133:501–9.
23. Yamabuki T, Takano A, Hayama S, et al. Dikkopf-1 as a novel serologic and prognostic biomarker for lung and esophageal carcinomas. Cancer Res 2007;67:2517–25.
24. Bloom HJ, Richardson WW. Histological grading and prognosis in breast cancer; a study of 1409 cases of which 359 have been followed for 15 years. Br J Cancer 1957;11:359–77.
25. Sakamoto G, Inaji H, Akiyama F, et al. General rules for clinical and pathological recording of breast cancer 2005. Breast Cancer 2005;12 Suppl:S1–27.
26. Takamura Y, Kobayashi H, Taguchi T, Motomura K, Inaji H, Noguchi S. Prediction of chemotherapeutic response by collagen gel droplet embedded culture-drug sensitivity test in human breast cancers. Int J Cancer 2002;98:450–5.
27. Kobayashi H. Development of a new *in vitro* chemosensitivity test using collagen gel droplet embedded culture and image analysis for clinical usefulness. Recent Results Cancer Res 2003;161:48–61.
28. Kobayashi H, Higashiyama M, Minamigawa K, et al. Examination of *in vitro* chemosensitivity test using collagen gel droplet culture method with colorimetric endpoint quantification. Jpn J Cancer Res 2001;92:203–10.
29. Wicha MS, Liu S, Dontu G. Cancer stem cells: an old idea—a paradigm shift. Cancer Res 2006; 66:1883–90, discussion 95–6.
30. Song LL, Miele L. Cancer stem cells—an old idea that's new again: implications for the diagnosis and treatment of breast cancer. Expert Opin Biol Ther 2007;7:431–8.
31. Jordan CT, Guzman ML, Noble M. Cancer stem cells. N Engl J Med 2006;355:1253–61.
32. Li X, Lewis MT, Huang J, et al. Intrinsic resistance of tumorigenic breast cancer cells to chemotherapy. J Natl Cancer Inst 2008;100:672–9.
33. Magni M, Shammah S, Schiro R, Mellado W, Dalla-Favera R, Gianni AM. Induction of cyclophosphamide-resistance by aldehyde-dehydrogenase gene transfer. Blood 1996;87: 1097–103.
34. Bear HD, Anderson S, Brown A, et al. The effect on tumor response of adding sequential preoperative docetaxel to preoperative doxorubicin and cyclophosphamide: preliminary results from National Surgical Adjuvant Breast and Bowel Project Protocol B-27. J Clin Oncol 2003;21: 4165–74.
35. Colleoni M, Viale G, Zahrieh D, et al. Chemotherapy is more effective in patients with breast cancer not expressing steroid hormone receptors: a study of preoperative treatment. Clin Cancer Res 2004;10:6622–8.
36. Estevez LG, Cuevas JM, Anton A, et al. Weekly docetaxel as neoadjuvant chemotherapy for stage II and III breast cancer: efficacy and correlation with biological markers in a phase II, multicenter study. Clin Cancer Res 2003;9:686–92.
37. Stearns V, Singh B, Tsangaris T, et al. A prospective randomized pilot study to evaluate predictors of response in serial core biopsies to single agent neoadjuvant doxorubicin or paclitaxel for patients with locally advanced breast cancer. Clin Cancer Res 2003;9:124–33.
38. Rody A, Karn T, Gatje R, et al. Gene expression profiling of breast cancer patients treated with docetaxel, doxorubicin, and cyclophosphamide within the GEPARTRIO trial: HER-2, but not topoisomerase IIα and microtubule-associated protein τ, is highly predictive of tumor response. Breast 2007;16:86–93.

Genetic Polymorphisms of CYP2D6*10 and CYP2C19*2,*3 Are not Associated With Prognosis, Endometrial Thickness, or Bone Mineral Density in Japanese Breast Cancer Patients Treated With Adjuvant Tamoxifen

Masatsugu Okishiro, MD, Tetsuya Taguchi, MD, Seung Jin Kim, MD, Kenzo Shimazu, MD, Yasuhiro Tamaki, MD, and Shinzaburo Noguchi, MD

BACKGROUND: The authors investigated the impact of the genetic polymorphisms cytochrome P450 (CYP) family 2, subfamily D, polypeptide 6, allele *10 (CYP2D6*10) and CYP family 2, subfamily C, polypeptide 19, allele *2,*3 (CYP2C19*2,*3) on disease recurrence in patients with breast cancer who received adjuvant tamoxifen and evaluated the impact of those polymorphisms on endometrial thickness, bone mineral density (BMD), and serum total cholesterol levels. **METHODS:** Patients with primary breast cancer (n=173) who had hormone receptor-positive tumors and who also received adjuvant tamoxifen were included in the current study. Genetic polymorphisms of CYP2D6*10 and CYP2C19*2,*3 were analyzed. **RESULTS:** Recurrence-free survival (RFS) rates did not differ significantly between patients with the CYP2D6 *10/*10 genotype (n=40) and patients with the CYP2D6 wild-type (wt)/wt or wt/*10 genotype (n=133) or between patients with the CYP2C19 *2/*2, *2/*3, or *3/*3 genotypes (n=41) and patients with the CYP2C19 wt/wt, wt/*2, or wt/*3 genotype (n=132). Multivariate analysis indicated that, even after adjustment for well established prognostic factors, these CYP2D6 or CYP2C19 genotypes were not associated significantly with the RFS rate. Moreover, these genotypes did not affect endometrial thickness, BMD, or total cholesterol levels 1 year after the start of tamoxifen treatment. **CONCLUSIONS:** Neither the CYP2D6 *10/*10 genotype nor the CYP2C19 genotype is likely to have a clinically significant impact on prognosis, endometrial thickness, BMD, or total cholesterol levels in Japanese patients with breast cancer who are treated with adjuvant tamoxifen. **Cancer 2009;115:952–61. © 2009 American Cancer Society.**

KEY WORDS: breast cancer, cytochrome P450 family 2, subfamily D, polypeptide 6, cytochrome P450 family 2, subfamily C, polypeptide 19, tamoxifen.

Corresponding author: Shinzaburo Noguchi, MD, Department of Breast and Endocrine Surgery, Osaka University Graduate School of Medicine, 2-2-E10 Yamadaoka, Suita City, Osaka 565-0871, Japan; Fax: (011) 81-6-6879-3779; noguchi@onsurg.med.osaka-u.ac.jp

Department of Breast and Endocrine Surgery, Osaka University Graduate School of Medicine, Osaka, Japan

Received: July 1, 2008; **Revised:** August 29, 2008; **Accepted:** September 19, 2008

Published online: January 20, 2009, © 2009 American Cancer Society

DOI: 10.1002/cncr.24111, www.interscience.wiley.com

Tamoxifen has been used widely as a standard treatment in metastatic and adjuvant settings for estrogen receptor (ER)-positive and/or progesterone receptor (PgR)-positive breast cancers.[1,2] Tamoxifen as such has a low affinity for ER but is metabolized to active forms, such as 4-hydroxytamoxifen (4OH-TAM) and endoxifen, which have approximately 100 times higher affinity for ER than tamoxifen.[3] This metabolic activation of tamoxifen is mediated mainly by cytochrome P450 (CYP) family 2, subfamily D, polypeptide 6 (CYP2D6) and by CYP family 3, subfamily A, polypeptide 4/5 (CYP3A4/5). CYP2D6 is a highly polymorphic gene, and it has been established that several of its genetic variants, such as the CYP2D6*3, CYP2D6*4, and CYP2D6*5 alleles, do not carry any enzymatic activity.[4,5] Furthermore, a recent study demonstrated that patients with breast cancer who carry 2 of these null alleles have reduced levels of 4OH-TAM and endoxifen[6] compared with patients who have the CYP2D6 wt/wt genotype.

It is noteworthy that, in another recent study, patients with breast cancer who had the CYP2D6 *4/*4 genotype had worse clinical outcomes than patients who had other genotypes, probably because of the reduced activation of tamoxifen.[7] This finding may have important clinical implications for Western countries, because the CYP2D6 *4/*4 genotype occurs in 5% to 10% of Caucasians. Conversely, this genotype is very rare among Asians (<1%); however, the CYP2D6 *10/*10 genotype, which carries reduced enzyme activity (about 10% of the activity of the wild allele homozygote),[8] is relatively common and is observed in 15% to 20% of Japanese.[5] Very recently, it was demonstrated that progression of metastatic breast cancer occurs significantly sooner in patients who have the CYP2D6 *10/*10 genotype when they are treated with tamoxifen than in patients who have the CYP2D6 wt/wt or wt/*10 genotype[9] and that the prognosis for breast cancer patients who are treated with adjuvant tamoxifen is worse for those who have the CYP2D6 *10/*10 genotype than for those who have the CYP2D6 wt/wt or wt/*10 genotype.[10,11] These results appear to suggest that a reduced metabolism of tamoxifen in patients with the CYP2D6 *10/*10 genotype is important clinically in affecting the response to tamoxifen.

In addition to these findings for the CYP2D6 polymorphism, a recent study indicated that patients with the CYP2C19 *17 allele, which has higher activity than the wt allele, had a better prognosis than patients without it, probably because of the enhanced metabolism of tamoxifen into 4OH-TAM and endoxifen.[12] Although the occurrence of CYP2C19 *17 allele carriers is very rare in Japanese (<1% in Japanese but about 10% in Caucasians),[8] the occurrence of the CYP2C19 *2/*2, *3/*3, or *2/*3 genotype (neither the *2 allele nor the *3 allele possesses enzyme activity) is relatively high, accounting for approximately 20% in Japanese.[13] It has been speculated that tamoxifen activation is reduced in patients who have these genotypes, resulting in high recurrence rates when they are treated with adjuvant tamoxifen, as reported for the CYP2D6 *4/*4 and CYP2D6 *10/*10 genotypes; whereas, to our knowledge, no studies have been reported on the relation between the CYP2C19 *2/*2, *2/*3, or *3/*3 genotype and recurrence rates.

For the report, we studied the impact not only of the CYP2D6 *10/*10 genotype but also of the CYP2C19 *2/*2, *3/*3, or *2/*3 genotype on recurrence rates in patients with breast cancer who were treated with adjuvant tamoxifen. In addition, we studied the impact of these genetic polymorphisms on endometrial thickness, bone mineral density (BMD), and serum cholesterol levels, because these variables also can be expected to influence the effects of tamoxifen on these target organs.

MATERIALS AND METHODS

Patients

Serial patients with primary breast cancer (n = 173), who had hormone receptor-positive (ER-positive and/or PgR-positive) tumors, underwent mastectomy or breast-conserving surgery between October 1998 and December 2004 and were treated with adjuvant tamoxifen (20 mg daily), were included in this study. The median follow-up was 56 months (range, 8-109 months), and the median duration of adjuvant tamoxifen treatment was 52 months (range, 9-60 months). Characteristics of these patients are shown in Table 1. Seventy-three patients received tamoxifen alone, and 100 patients received tamoxifen, chemotherapy, and/or goserelin. Chemotherapy comprised either 6 cycles of combined oral cyclophosphamide (100 mg daily

Table 1. Characteristics of Patients Included in This Study

Characteristic	All Patients, n=173	CYP2D6 Wt/Wt or Wt/*10, n=133	CYP2D6 *10/*10, n=40	CYP2D6 P	CYP2C19 EM, n=132	CYP2C19 PM, n=41	CYP2C19 P
Median age (range), y	47 (22-73)	47 (22-72)	46 (27-73)	.47	47 (27-73)	47 (22-69)	.64
Menopausal status				**.59**			**.51**
Premenopausal	135	105	30		104	31	
Postmenopausal	38	28	10		28	10	
Tumor size, cm				**.81**			**.75**
≤2	98	76	22		75	23	
>2	75	57	18		57	18	
Lymph node status				**.82**			**.72**
Positive	50	39	11		36	14	
Negative	123	94	29		96	27	
ER status				**.47**			**.94**
Positive	157	123	34		120	37	
Negative	16	10	6		12	4	
PgR status				**.94**			**.52**
Positive	148	114	34		115	33	
Negative	25	19	6		17	8	
HER-2 status				**.44**			**.71**
Positive	13	9	4		11	2	
Negative	119	96	23		89	30	
Unknown	41	28	13		32	9	
Histologic grade				**.84**			**.54**
1	49	38	11		37	12	
2	119	91	28		90	29	
3	5	4	1		5	0	
Adjuvant treatment				**.88**			**.95**
TAM	73	56	17		57	16	
TAM and others†	100	77	23		75	25	

CYP2D6 indicates cytochrome P450 family 2, subfamily D, polypeptide 6; CYP2C19, cytochrome P450 family 2, subfamily C, polypeptide 19; Wt, wild-type allele; *10, allele *10; EM, extensive metabolizers; PM, poor metabolizers; ER, estrogen receptor; PgR, progesterone receptor; HER-2, human epidermal growth factor receptor 2; TAM, tamoxifen.
† Chemotherapy and/or goserelin.

on Days 1-14), intravenous methotrexate (40 mg/m^2 on Days 1 and 8), and intravenous 5-fluouroracil (5-FU) (600 mg/m^2 on Days 1 and 8; n = 8 patients); or 4 cycles of intravenous cyclophosphamide (600 mg/m^2 on Day 1) and intravenous epirubicin (60 mg/m^2 on Day 1; n = 32 patients); or others (n = 2 patients). Goserelin (3.75 mg every 4 weeks; n = 58 patients) was administered for 2 years. The patients who received paroxetine (a selective serotonin reuptake inhibitor [SSRI]) concomitantly with tamoxifen were excluded, because SSRIs are potent inhibitors of CYP2D6.[14,15] Informed consent was obtained from all patients.

Genotype Analysis

In brief, DNA was extracted from peripheral whole blood mononuclear cells and was subjected to TaqMan single-nucleotide polymorphism (SNP) Genotyping Assays (Applied Biosystems, Foster City, Calif) for identification of the CYP2D6 *10 allele. Polymerase chain reaction (PCR) was performed on the ABI prism 7900HT (Applied Biosystems) at 95°C for 10 minutes followed by 50 cycles at 92°C for 15 seconds and at 60°C for 90 seconds; and the fluorescent signal was detected by the ABI prism 7900HT (Applied Biosystems). The CYP2C19 *2

and *3 alleles were identified by using TaqMan SNP Genotyping Assays (Applied Biosystems). PCR was performed on the ABI prism 7900HT (Applied Biosystems) at 95°C for 5 minutes followed by 50 cycles at 92°C for 15 seconds and at 60°C for 90 seconds; and the fluorescent signal was detected by the ABI prism 7900HT (Applied Biosystems). Because the CYP2C19 *2 and *3 alleles do not have enzyme activity, patients with the CYP2C19 *2/*2, *2/*3, or *3/*3 genotypes were designated as poor metabolizers (PMs), and patients with the CYP2C19 wt/wt, wt/*2, or wt/*3 genotypes were designated as extensive metabolizers (EMs).[8,13,14]

Estrogen Receptor, Progesterone Receptor, and Human Epidermal Growth Factor Receptor 2

ER and PgR levels were defined as positive by immunohistochemistry (IHC) when ≥10% of tumor cells stained positive for these receptors (ER, clone 6F11; PgR, clone 16; Ventana Japan K.K. and SRL Inc., Tokyo, Japan). Human epidermal growth factor receptor 2 (HER-2) levels were determined by fluorescence in situ hybridization (FISH) using PathVysion Her-2 DNA Probe kits (SRL Inc.) or by IHC using the DAKO system scale (DAKO Diagnostics, Tokyo, Japan). When FISH indicated that a tumor contained >2 genes per cell or IHC indicated 3+ HER-2 staining, the tumor was considered HER-2-positive.

Recurrence-free Survival

To calculate RFS rates, distant recurrences, locoregional recurrences, ipsilateral in-breast recurrences, and contralateral breast cancers were included. RFS rates were estimated with the Kaplan-Meier method, and statistical significance was assessed with the log-rank test. Cox proportional hazard analyses (unadjusted and adjusted) also were performed.

Bone Mineral Density, Endometrial Thickness, and Total Cholesterol Levels

The influence of tamoxifen on BMD, endometrial thickness, and total cholesterol was studied in postmenopausal patients according to genotype (CYP2D6*10 or CYP2C19*2,*3). BMD of the lumbar spine (lumbar segments 2-4 [L2-L4]) was measured by using a dual-energy x-ray absorptiometer (Lunar DPX; GE Medical Systems, Tokyo, Japan) in 20 patients, and endometrial thickness was measured by transvaginal ultrasonography (SONOVISTA MSC; Siemens AG, Beyer, Munich, Germany) in 21 patients at baseline and 1 year after the start of tamoxifen. Total serum cholesterol levels also were measured by using the cholesterol oxidase method in 30 patients at baseline and 1 year after the start of tamoxifen. Changes from baseline in lumbar spine BMD, endometrial thickness, and cholesterol levels were assessed with the *t* test for paired data.

Statistical Analysis

Statview software (version 5.0 for Windows; SAS Institute Inc., Cary, NC) was used for statistical analyses. A *P* value <.05 was considered statistically significant.

RESULTS

Frequencies of CYP2D6*10 or CYP2C19*2,*3 Genotype and Relation With Clinicopathologic Features of Breast Tumors

TaqMan SNP genotyping assays were used to identify CYP2D6 and CYP2C19 genotypes in 173 patients. The frequency of the CYP2D6 *10/*10 genotype was 23.1%, and the frequency of the CYP2D6 wt/wt or wt/*10 genotype was 76.9%. The frequency of the CYP2C19 *2/*3, *2/*2, or *3/*3 genotype (ie, PMs) was 23.7%; and the frequency of the CYP2C19 wt/wt, wt/*2, or wt/*3 genotype (ie, EMs) was 76.3% (Table 2). None of these genotypes showed any significant association with various clinicopathologic parameters, including menopausal status, tumor size, lymph node status, ER, PgR, HER-2, histologic grade, and type of adjuvant therapy (Table 1).

Recurrence-free Survival Rates by CYP2D6*10 Genotype

RFS rates were not significantly different between patients with the CYP2D6 *10/*10 genotype (median follow-up, 63 months; range, 23-96 months; n = 40) and those with the wt/wt or wt/*10 genotype (median follow-up, 54 months; range, 8-109 months; n = 133; log-rank test;

$P = .98$) (Fig. 1a). When the analysis was limited to 73 patients who received adjuvant tamoxifen alone, again, there was no significant difference in RFS rates between these groups (log-rank test; $P = .57$) (Fig. 1b). Multivariate analysis indicated that, even after adjustment for well established prognostic factors such as tumor size, lymph node status, histologic grade, ER, and PgR, there still was no significant difference in RFS rates between patients with the CYP2D6 *10/*10 genotype and those with the CYP2D6 wt/wt or wt/*10 genotype (Table 3).

Table 2. Genotype Frequency of the Cytochrome P450 (CYP) 2D6*10 and CYP2C19*2,*3 Polymorphisms

Genotype	No. of Patients, n=173	%
CYP2D6		
Wt/Wt	74	42.8
Wt/*10	59	34.1
*10/*10	40	23.1
CYP2C19		
*1/*1	53	30.6
*1/*2	56	32.4
*1/*3	23	13.3
*2/*3	17	9.8
*2/*2	20	11.6
*3/*3	4	2.3

CYP2D6 indicates cytochrome P450 family 2, subfamily D, polypeptide 6; Wt, wild-type allele; *10, allele *10; CYP2C19, cytochrome P450 family 2, subfamily C, polypeptide 19.

*Recurrence-free Survival Rates by CYP2C19*2,*3 Genotype*

RFS rates did not differ significantly for the CYP2C19 PM genotypes (*2/*2, *2/*3, or *3/*3; median follow-up, 63 months; range, 36-109 months) and the EM genotypes (wt/wt, wt/*2, or wt/*3; median follow-up, 54 months; range, 8-109 months; log-rank test; $P = .19$) (Fig. 2a). When the analysis was limited to 73 patients who received adjuvant tamoxifen alone, again, there was no significant difference in RFS rates between these 2 groups (log-rank test; $P = .47$) (Fig. 2b). Multivariate analysis indicated that, after adjustment for the same prognostic factors described above, again, there was no significant difference in RFS rates between the CYP2C19 EM and PM genotypes (Table 3).

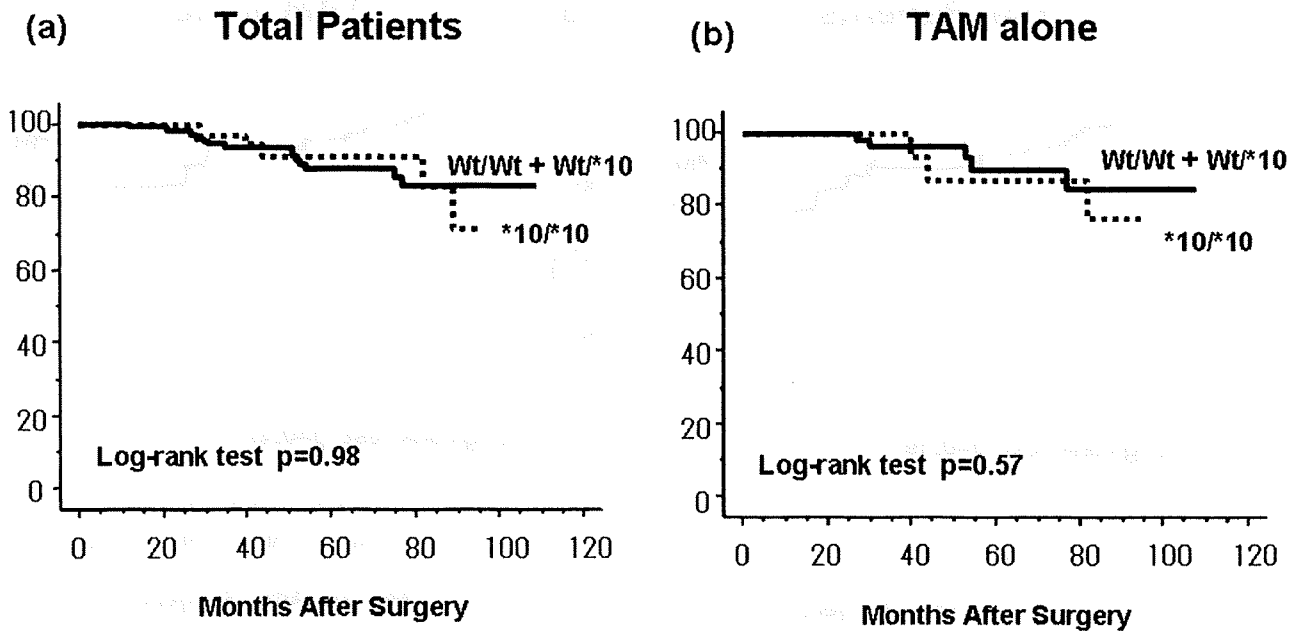

FIGURE 1. The prognosis of patients who received adjuvant tamoxifen according to cytochrome P450 (CYP) family 2, subfamily D, polypeptide 6, allele *10 (CYP2D6*10) genotype. Recurrence-free survival rates were calculated with the Kaplan-Meier method according to CYP2D6 genotype, ie, the CYP2D6 *10/*10 genotype and the CYP2D6 wild-type (wt)/wt or wt/*10 genotype, for all patients who received adjuvant tamoxifen (a) and for patients who received adjuvant tamoxifen alone (b).